

Article

Assessing the Calibration of Benthic Foraminifera Elemental Ratios from the Northeastern Atlantic

Sophie Sepulcre ^{1,*}, Marion Tribondeau ¹, Franck Bassinot ², Meryem Mojtahid ³, Maria-Pia Nardelli ³, Pierre-Antoine Dessandier ^{4,5} and Jérôme Bonnin ⁵

¹ Université Paris-Saclay, CNRS, GEOPS, Rue du Belvédère, Bât. 504, 91405 Orsay, France; marion91_t@hotmail.fr

² IPSL-LSCE, CEA CNRS UVSQ, UMR 8212, 91190 Gif Sur Yvette, France; franck.bassinot@lsce.ipsl.fr

³ Université d'Angers, Université de Nantes, Université Le Mans, CNRS, LPG, UMR 6112, 2 Bd Lavoisier, 49045 Angers Cedex, France; meryem.mojtahid@univ-angers.fr (M.M.); mariapia.nardelli@univ-angers.fr (M.-P.N.)

⁴ Université de Bordeaux, CNRS, UMR 5805 EPOC, 33615 Pessac, France

⁵ Université de Brest, CNRS, Ifremer, UMR 6197, 29280 Plouzané, France;

pierre.antoine.dessandier@ifremer.fr (P.-A.D.); jerome.bonnin@u-bordeaux.fr (J.B.)

* Correspondence: sophie.sepulcre@universite-paris-saclay.fr

Abstract: On six different species of benthic foraminifera covering various microhabitats and recovered from the Northern Atlantic Ocean, we tested the potential of the Mg/Ca and Sr/Ca ratios as proxies for paleoceanography. We performed analysis using two instruments (ICP-OES and ICP-MS) and compared results obtained from living and dead specimens. Our results are in good agreement with previous published calibrations for *Hoeglundina elegans*, *Uvigerina mediterranea*, *U. peregrina*, *Melonis barleeanum*, and *Globobulimina* spp. However, we observed a strong variability between living and dead specimens, and between both instrumental approaches. We discuss the impact of the cleaning procedure, as well as the natural variability between samples recovered at different depths inside the sediment. No specific trend can be deciphered from our dataset, but we observed that species from the *Uvigerina* genus presented the lowest external reproducibility and the best agreement between living and dead specimens. We highlight that both species should not be mixed for analysis, since *U. mediterranea* presents lower values and a reduced range of variability compared to *U. peregrina*. We explored the temperature and the $\Delta[\text{CO}_3^{2-}]$ as potential controls on the variability of both ratios from *U. peregrina* and showed that neither of these two parameters can be discarded.

Keywords: benthic foraminifera; Bay of Biscay; elemental ratio; bottom water temperature; carbonate concentration



Citation: Sepulcre, S.; Tribondeau, M.; Bassinot, F.; Mojtahid, M.; Nardelli, M.-P.; Dessandier, P.-A.; Bonnin, J. Assessing the Calibration of Benthic Foraminifera Elemental Ratios from the Northeastern Atlantic. *J. Mar. Sci. Eng.* **2024**, *12*, 736. <https://doi.org/10.3390/jmse12050736>

Academic Editor: Rocco Gennari

Received: 1 March 2024

Revised: 5 April 2024

Accepted: 6 April 2024

Published: 28 April 2024



Copyright: © 2024 by the authors. Licensee MDPI, Basel, Switzerland. This article is an open access article distributed under the terms and conditions of the Creative Commons Attribution (CC BY) license (<https://creativecommons.org/licenses/by/4.0/>).

1. Introduction

Reconstructing past climates is a key step towards understanding the current climate system and its future evolution [1,2]. Except for a few cases, such as ice cores, in which direct measurements can be made (e.g., [3]), most climate reconstructions rely on proxies, which make it possible to reproduce the variability of an environmental parameter over time (e.g., [4–6]). Consequently, the calibration of these tracers under known (e.g., modern environment) and/or controlled (e.g., laboratory) conditions is an essential prerequisite for their application to climate archives.

In the ocean, calcium carbonates CaCO_3 recovered from marine sediments are well-studied archives for reconstruction of past changes in the physical and chemical seawater properties related to ocean dynamics and circulation, and, in a larger sense, to global climate changes. In particular, the relationship between the concentration of some elements—normalized to Ca—and environmental parameters has been explored, both through laboratory experiments on these abiotic CaCO_3 (e.g., [7]) and on biogenic CaCO_3 (e.g., [8]). Moreover, instrumental development since the 1980s has enabled the chemical

composition of climate archives to be measured with increasing precision on ever smaller sample quantities (e.g., [9–17]).

Foraminifera, which are unicellular organisms, secrete a CaCO_3 test, potentially recording in their geochemical signature the parameters of the environment in which they precipitated their test. Because of the chemical composition of their tests and their ecological preferences, foraminifera, like other groups of micro- or nanofossils, are powerful archives of environmental change (e.g., [18,19]). Benthic foraminifera especially live at the water-sediment interface (epifaunal species) or deeper inside the sediment (endofaunal species). This distribution mainly depends on the quantity and quality of the organic matter that sediments contain, as well as oxygen availability (TROX model, [20,21]). They represent a key microfossil group to reconstruct past changes in the deep-water properties and dynamics through time.

Among the various environmental parameters, the reconstruction of the temperature of bottom water (Bottom-Water Temperature, BWT) masses has been widely explored. Indeed, constraining variations in ocean temperature is a key factor to better assess exchanges between the different water masses as well as between the reservoirs of the climate system and the variations in their dynamics. To achieve this objective, the Magnesium to Calcium ratio Mg/Ca has been studied since the 1990s and has rapidly become a key tracer in palaeoceanographic reconstructions when the relationship between this elemental ratio and temperature was demonstrated in planktonic foraminifera by the pioneering work of, for example, [22–25] and also in benthic foraminifera [26]. Numerous studies have since refined these relationships in benthic foraminifera based on the analysis of core tops (e.g., [27–33]) or laboratory culture experiments (e.g., [33–41]). Nevertheless, limitations have also gradually been highlighted, such as (i) the impact of other environmental parameters on the Mg/Ca tracer, and especially the carbonate ion content [CO_3^{2-}] (or associated parameters like $\Delta[\text{CO}_3^{2-}]$ or Ω) [28,42] and (ii) the impact of different cleaning protocols and the choice of calibration applied on the results [28,41,43,44].

To better understand the sources of Mg/Ca vs. temperature deviation, coupling with other proxies may be useful. Several studies have explored the potential of the Strontium versus Calcium (Sr/Ca) proxy, which shows a relationship with carbonate system parameters in inorganic precipitation experiments [45–47] but also in cultured benthic foraminifera [34,48,49] or modern foraminifera [45–47,50]. However, these results are controversial since other works did not find any relationships between the Sr/Ca and the carbonate system parameters; in conclusion, other studies on benthic foraminifera have shown that there is no relationship between Sr/Ca and the temperature or salinity of deep waters (e.g., [51,52]).

The present work aims at refining the relationships between the Mg/Ca and the Sr/Ca ratios with the BWT and the $\Delta[\text{CO}_3^{2-}]$ for several species of benthic foraminifera recovered in modern sediments from the Northern Atlantic Ocean, a key area for the Atlantic Meridional Overturning Circulation (AMOC) and climate regulation (e.g., [53,54]). Our aim is to combine the existing Mg/Ca and Sr/Ca calibrations with our new data to refine these calibrations and help in obtaining more precise palaeoceanographic reconstructions. Indeed, there is no real consensus on the calibration to choose for BWT reconstructions (e.g., [30,31] and references therein), and environmental controls on the Mg/Ca and the Sr/Ca variations are still under debate (e.g., [31,48]). To achieve these goals, we analyze six benthic foraminiferal species from the Bay of Biscay living at water depths from 250 to 1993 m covering various BWT (4.1–11.8 °C; [55]) and $\Delta[\text{CO}_3^{2-}]$ conditions ($\Delta[\text{CO}_3^{2-}]_{\text{calcite}} = 72.6\text{--}99.2 \mu\text{mol. mol}^{-1}$) (Figure 1). We also test two technical approaches to measure the Mg/Ca and Sr/Ca ratios. When possible, we compare the results obtained from living specimens (i.e., Rose Bengal-stained) with dead individuals. Finally, we discuss the potential control of BWT and $\Delta[\text{CO}_3^{2-}]$ on both proxies and compile our data with the existing published datasets.

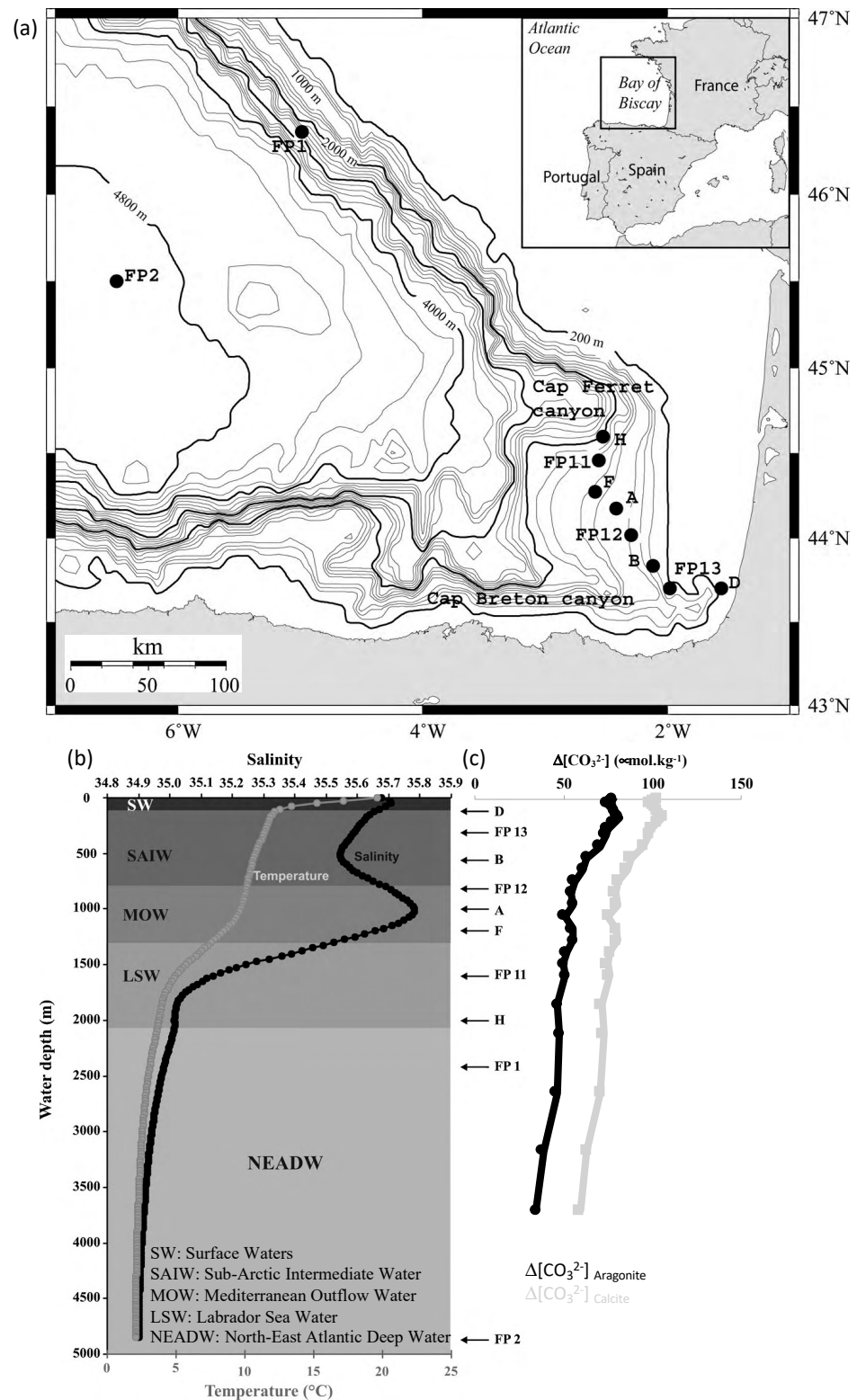


Figure 1. (a) Study site and location of sampling stations and current hydrological data: profiles of (b) Temperature (grey) and Salinity (black) and (c) $\Delta[\text{CO}_3^{2-}]$ of calcite (black) and aragonite (grey) calculated with CO2.SYS.EXE software [56] and the WOCE database [57]. Modified from [55].

2. Study Area

The Bay of Biscay is largely open to the North Atlantic and is, therefore, subject to the influence of the North Atlantic surface circulation (Figure 1).

Surface water (Figure 1) representing the eastern edge of a branch of the North Atlantic current, the Eastern North Atlantic Central Water (ENACW), flows from the north, along the Irish plateau, southwards to Cape Finisterre, and is characterized by highly variable temperatures and salinity depending on the season [58]. Between ~150 and 800 m below the surface, the SAIW (Sub Arctic Intermediate Water) mass circulates, with salinities decreasing from 35.65 to 35.5 psu and temperatures decreasing slightly from around 12 to 10 °C (Figure 1; [59–61]). Between ~800 and 1200 m, the increase in salinity from 35.65 to 35.8 psu marks the influence of the Mediterranean Outflow Water (MOW) with temperatures from 7.5 to 10 °C (Figure 1; [59–61]). The underlying water mass, the Labrador Sea Water (LSW), is characterized by much lower salinities (from 35.6 to 35.0 psu) and temperatures of between 4 and 7 °C. Deeper, the North Atlantic Deep Water (NADW) is found, with salinities and temperatures decreasing slightly (from 35.0 to 34.9 psu and from 4 to 2 °C, respectively) (Figure 1; [59–61]).

These different water masses are also characterized by varying states of saturation with respect to calcite and aragonite, represented by the $\Delta[\text{CO}_3^{2-}]$ [62] (Equation (1)):

$$\Delta[\text{CO}_3^{2-}] = [\text{CO}_3^{2-}]_{\text{in situ}} - [\text{CO}_3^{2-}]_{\text{saturation}} \tag{1}$$

which corresponds to the difference between the $[\text{CO}_3^{2-}]$ concentration in the water and the $[\text{CO}_3^{2-}]$ concentration at saturation defined as (Equation (2)):

$$[\text{CO}_3^{2-}]_{\text{saturation}} = \frac{[\text{CO}_3^{2-}]_{\text{in situ}}}{\Omega} \tag{2}$$

where Ω is the saturation defined by the ratio (Equation (3)):

$$\Omega = \frac{[\text{CO}_3^{2-}] \times [\text{Ca}^{2+}]}{K_{\text{sp}}} \tag{3}$$

where K_{sp} is the solubility product of aragonite or calcite. When $\Omega < 1$ or >1 , the waters are undersaturated and oversaturated with respect to CaCO_3 , respectively.

Calculations of $\Delta[\text{CO}_3^{2-}]$ using the CO2SYS software [56] with the WOCE database [57] show that the waters in the Bay of Biscay are supersaturated with respect to calcite and aragonite throughout the depth range, attesting to good preservation conditions at the study site (Figure 1c).

The main environmental parameters of the stations studied are summarized in Table 1.

Table 1. Main characteristics of the stations studied. Values marked * are estimated from the WOCE database [57] and not measured in situ.

Station	Location		Depth (m)	T(°C)	Salinity (psu)	[O ₂] (mmol.L ⁻¹)	$\Delta[\text{CO}_3^{2-}]_{\text{calcite}}$ mmol.mol ⁻¹	$\Delta[\text{CO}_3^{2-}]_{\text{aragonite}}$ mmol.mol ⁻¹
C	43°40'08 N	1°38'87 W	250	11.8	35.6 *	225	99.2	74.5
FP13	43°42'21 N	1°59'56 W	375	11.4	35.6	218	95.8	71.2
G	43°40'20 N	1°36'40 W	400	11.3	35.6 *	222	95.0	70.3
B	43°50'31 N	2°03'47 W	550	10.8	35.6	210	86.8	62.1
K	44°32'52 N	3°37'23 W	650	10.5*	35.6 *	202	72.6	55.2
E	43°46'06 N	1°48'03 W	750	10.4	35.7 *	199	79.9	54.4
FP12	43°59'98 N	2°15'12 W	800	10.2	35.7	175	79.1	50.8
A	44°10'24 N	2°20'06 W	1000	9.7	35.8	195	75.5	49.4
FP11	44°27'76 N	2°39'46 W	1600	5.8	35.3	250	74.0	47.9
WH	43°37'73 N	1°43'62 W	1993	4.1	35.1	261	72.6	47.9

3. Materials and Methods

Previous work has determined the benthic foraminiferal assemblages in the study area [55,63,64]. According to their findings, we selected six species: *Hoeglundina elegans* (the only one in aragonite shell) and *Hyalinea balthica* from the epifauna, *Uvigerina peregrina*, *U. mediterranea* and *Melonis barleeanum* from the superficial to intermediate endofauna, and *Globobulimina* spp. from the deep endofauna. The choice of species was guided by their abundance but also by the availability of previous geochemical data to be compared to (see references in the description of results). In addition, we selected species corresponding to different microhabitats, and it was possible to analyze living and dead specimens at the time of sampling, sometimes at the same station (see Table 2). The living specimens are recognized thanks to their pink color due to the Rose Bengal staining commonly used to identify live foraminifera [65].

Table 2. Analysis strategy applied. The first number corresponds to the number of different depths inside the sediment analyzed per station for each species and at each station. The number in brackets corresponds to the number of analyses (i.e., replicates) carried out per level. The letters “L” and “D” refer to live and dead specimens, respectively.

Station	Depth (m)	<i>H. elegans</i>		<i>H. balthica</i>		<i>U. mediterranea</i>		<i>U. peregrina</i>		<i>M. barleeanum</i>		<i>Globobulimina</i> spp.	
		L	D	L	D	L	D	L	D	L	D	L	D
C	250									1(*1) + 1(*2)		1(*2)	
FP13	375									1(*1)		1(*1)	
G	400							1(*2)					
B	550	3(*1)	1(*4)	1(*4) + 1(*2)		1(*2)	1(*3)	2(*1)	2(*1)		1(*1)		1(*1)
K	650										1(*1)	1(*1)	1(*1)
E	750											1(*1)	
FP12	800					1(*3)							
A	1000					1(*3) + 1(*1)	1(*4)	1(*1)	1(*2)		1(*1)	1(*1)	1(*1)
FP11	1600	1(*3)						1(*2)	1(*2)				
WH	1993	1(*2) + 1(*1)	1(*2)						1(*3)				

Around 10–15 foraminifera were picked from the coarse fraction (>150 µm) to reach a weight of around 250 µg. The samples were cleaned following the protocol of [43] and analyzed using two techniques, with an inductively coupled plasma optical emission spectrophotometer (ICP-OES) Varian Vista Pro AX at the LSCE following the analytical procedures developed by [9] (see also [66]), and with a high resolution inductively coupled plasma mass spectrometer (ICP-MS-HR) Thermo Element XR at GEOPS following the procedures of [17] (see also [50]). In order to overcome the Ca matrix effect, for the two approaches, two series of analyses were carried out, the first by aligning the samples at concentrations of 100 ppm and 1 ppm for ICP-OES and ICP-MS-HR, respectively, estimated from the weights of foraminifera and dedicated to measuring the real Ca concentration. The second series was used to precisely align the concentrations. Three alignments were made, one at 15 ppm plus another at 40 ppm for ICP-OES, and a single alignment at 45 ppm for ICP-MS-HR. Concentrations were determined through the intensity ratio calibration procedure from five standard solutions of appropriate concentrations for the two runs, that were gravimetrically prepared by spiking a 1000 ppm Ca standard with appropriate amounts of Mg, Sr, Fe, and Mn mono-elemental 1000 ppm certified grade stock solutions. Dilution of the standards and samples was done using ultra-pure 0.1 N HNO₃ that was analyzed as a blank. Raw intensities (including standards) were corrected by removing the

specific blank intensity values. Regular measurement of a sample of known composition was used to control instrument drift over time by bracketing, and the linear regression estimated using standards was interspersed every four samples. Standard curves were used to calculate elemental/Ca ratios, and coefficients of determination (r^2) were always >0.9999 for all elemental ratios.

The standard deviations are 1.3% and 1% for the Mg/Ca and Sr/Ca ratios and 1.1% and 0.8% for the Mg/Ca and Sr/Ca ratios respectively for ICP-OES and ICP-MS-HR. In addition, the measurement of other elements (in particular, Fe and Mn) enables us to monitor the efficiency of the cleaning protocol and, in particular, the elimination of clays and any contamination by oxy(hydroxy)des. The standard deviations are 5.0% and 7.2% on ICP-OES and 5% and 1.1% on ICP-MS-HR for the Mn/Ca and Fe/Ca ratios, respectively.

4. Results

4.1. Global Overview

All the results are shown in Table 3 and Figure 2.

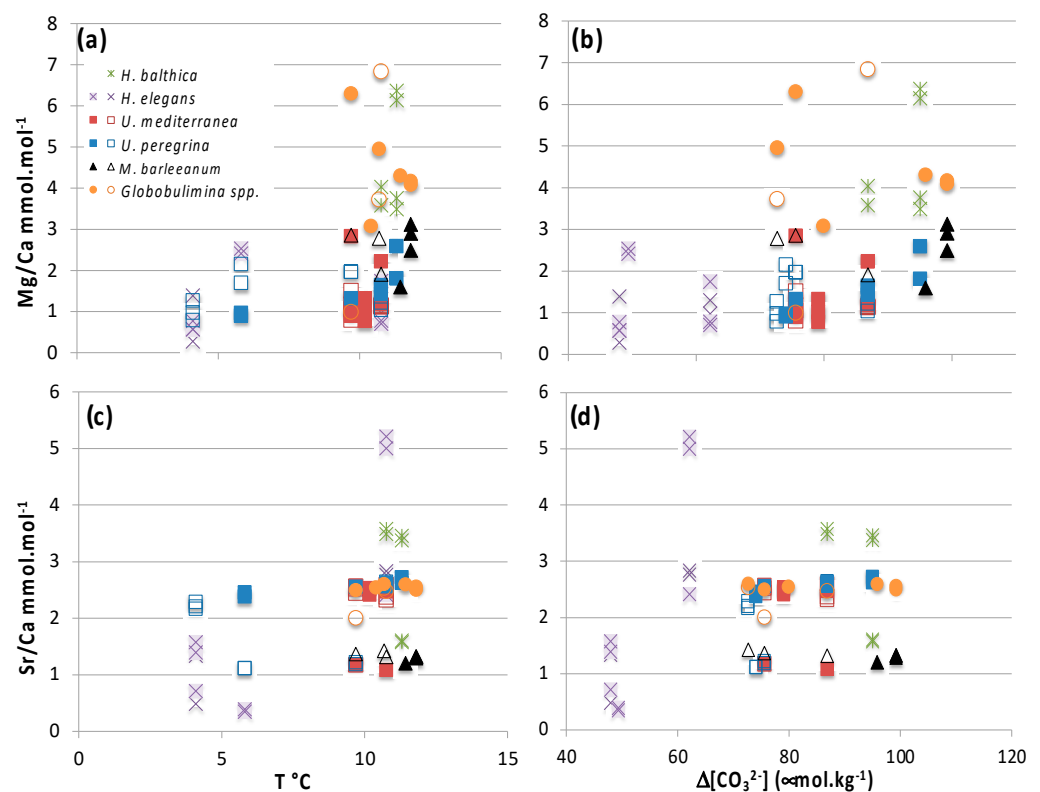


Figure 2. Variations in Mg/Ca (a,b) and Sr/Ca (c,d) versus temperature (a,c) and $\Delta[\text{CO}_3^{2-}]$ (b,d). Empty and full symbols represent data obtained from dead and live specimens, respectively. Green crosses: *Hyalinea balthica*; purple squares and crosses: *Hoeglundina elegans*; red squares: *Uvigerina mediterranea*; blue squares: *Uvigerina peregrina*; black triangles: *Melonis barleeanum*; orange circles: *Globobulimina* spp.

By applying selection criteria of Mn/Ca $<0.1 \text{ mmol}\cdot\text{mol}^{-1}$ and Fe/Ca $<0.1 \text{ mmol}\cdot\text{mol}^{-1}$ [43] (Table A1), only one sample of *M. barleeanum* for which the values were above the threshold was discarded (station B, level 1–1.5 cm, living specimen). The Mg/Ca and Sr/Ca values were plotted as a function of temperature (Figure 2a,c) and $\Delta[\text{CO}_3^{2-}]$ (Figure 2b,d) at the sampling station.

To clarify the description, the results are presented following the different microhabitats of the species.

Table 3. Results of elemental analyses carried out by ICP-OES (X) and ICP-MS-HR (*) on live (L) and dead (D) benthic foraminifera in the Bay of Biscay. See reference for stations in Table 1 and their location in Figure 1a.

Station	Water Depth (m)	Species	D/L	Depth inside the Sediment (cm)	Mg/Ca	1 s	Sr/Ca	1 s	Instrument
B	550	<i>H. elegans</i>	L	0.5–1	2.416	0.027	1.741	0.014	*
B	550	<i>H. elegans</i>	L	1–1.5	0.778	0.010	5.213	0.052	X
B	550	<i>H. elegans</i>	L	1.5–2	0.701	0.009	5.005	0.050	X
B	550	<i>H. elegans</i>	D	2–2.5	0.969	0.013	2.764	0.028	X
B	550	<i>H. elegans</i>	D	2–2.5	1.297	0.017	2.835	0.028	X
B	550	<i>H. elegans</i>	D	2–2.5	1.292	0.014	5.165	0.041	*
FP11	1600	<i>H. elegans</i>	L	0–0.5	2.533	0.033	0.393	0.004	X
FP11	1600	<i>H. elegans</i>	L	0–0.5	2.411	0.031	0.352	0.004	X
FP11	1600	<i>H. elegans</i>	L	0–0.5	1.117	0.012	0.646	0.005	*
WH	1993	<i>H. elegans</i>	L	0–0.5	0.573	0.007	1.394	0.014	X
WH	1993	<i>H. elegans</i>	L	0–0.5	0.771	0.010	1.578	0.016	X
WH	1993	<i>H. elegans</i>	D	0–0.5	0.278	0.004	1.338	0.013	X
WH	1993	<i>H. elegans</i>	D	0–0.5	1.385	0.015	0.485	0.004	*
WH	1993	<i>H. elegans</i>	L	0.5–1	0.715	0.008	0.574	0.005	*
G	400	<i>H. balthica</i>	L	0–0.5	3.486	0.045	3.377	0.034	X
G	400	<i>H. balthica</i>	L	0–0.5	3.756	0.049	3.460	0.035	X
G	400	<i>H. balthica</i>	L	0–0.5	6.366	0.070	1.579	0.013	*
G	400	<i>H. balthica</i>	L	0–0.5	6.143	0.068	1.607	0.013	*
B	550	<i>H. balthica</i>	L	1–1.5	4.029	0.052	3.578	0.036	X
B	550	<i>H. balthica</i>	L	1–1.5	3.581	0.047	3.489	0.035	X
B	550	<i>U. mediterranea</i>	L	0–0.5	1.174	0.015	2.472	0.025	X
B	550	<i>U. mediterranea</i>	L	0–0.5	1.087	0.012	1.517	0.012	*
B	550	<i>U. mediterranea</i>	D	1–1.5	1.126	0.015	2.325	0.023	X
B	550	<i>U. mediterranea</i>	D	1–1.5	1.127	0.015	2.594	0.026	X
B	550	<i>U. mediterranea</i>	D	1.5–2	1.148	0.013	2.375	0.019	*
FP12	800	<i>U. mediterranea</i>	L	0–0.5	0.776	0.010	2.410	0.024	X
FP12	800	<i>U. mediterranea</i>	L	0–0.5	1.319	0.017	2.533	0.025	X
FP12	800	<i>U. mediterranea</i>	L	0–0.5	1.014	0.013	2.506	0.025	X
A	1000	<i>U. mediterranea</i>	L	0–0.5	1.059	0.014	2.572	0.026	X
A	1000	<i>U. mediterranea</i>	L	0–0.5	0.898	0.012	2.556	0.026	X
A	1000	<i>U. mediterranea</i>	L	0–0.5	0.959	0.012	2.546	0.025	X
A	1000	<i>U. mediterranea</i>	L	0.5–1	1.170	0.013	2.835	0.023	*
A	1000	<i>U. mediterranea</i>	D	1–1.5	1.179	0.015	2.563	0.026	X
A	1000	<i>U. mediterranea</i>	D	1–1.5	1.055	0.014	2.446	0.024	X
A	1000	<i>U. mediterranea</i>	D	1–1.5	0.800	0.010	2.523	0.025	X
A	1000	<i>U. mediterranea</i>	D	1–1.5	1.173	0.013	1.506	0.012	*
G	400	<i>U. peregrina</i>	L	0–0.5	1.808	0.024	2.724	0.027	X
G	400	<i>U. peregrina</i>	L	0–0.5	2.589	0.034	2.624	0.026	X
B	550	<i>U. peregrina</i>	L	0–0.5	1.638	0.021	2.563	0.026	X
B	550	<i>U. peregrina</i>	L	0.5–1	1.598	0.021	2.588	0.026	X
B	550	<i>U. peregrina</i>	D	0.5–1	1.216	0.016	2.646	0.026	X
B	550	<i>U. peregrina</i>	L	1–1.5	1.430	0.019	2.630	0.026	X
B	550	<i>U. peregrina</i>	D	1–1.5	1.039	0.014	2.593	0.026	X
A	1000	<i>U. peregrina</i>	L	0–0.5	1.317	0.017	2.557	0.026	X
A	1000	<i>U. peregrina</i>	D	5.5–6.5	1.966	0.022	1.185	0.009	*
A	1000	<i>U. peregrina</i>	D	5.5–6.5	1.970	0.022	1.222	0.010	*
FP11	1600	<i>U. peregrina</i>	L	1–1.5	0.900	0.012	2.381	0.024	X

Table 3. Cont.

Station	Water Depth (m)	Species	D/L	Depth inside the Sediment (cm)	Mg/Ca	1 s	Sr/Ca	1 s	Instrument
FP11	1600	<i>U. peregrina</i>	L	1–1.5	0.968	0.013	2.456	0.025	X
FP11	1600	<i>U. peregrina</i>	D	3–3.5	2.149	0.024	1.120	0.009	*
FP11	1600	<i>U. peregrina</i>	D	3–3.5	1.701	0.019	1.118	0.009	*
WH	1993	<i>U. peregrina</i>	D	0–0.5	1.271	0.017	2.169	0.022	X
WH	1993	<i>U. peregrina</i>	D	0–0.5	0.976	0.013	2.207	0.022	X
WH	1993	<i>U. peregrina</i>	D	0–0.5	0.791	0.010	2.290	0.023	X
C	250	<i>M. barleaanum</i>	L	0.5–1	3.121	0.034	1.324	0.011	*
C	250	<i>M. barleaanum</i>	L	5–6	2.903	0.032	1.327	0.011	*
C	250	<i>M. barleaanum</i>	L	5–6	2.487	0.027	1.292	0.010	*
FP13	375	<i>M. barleaanum</i>	L	1–1.5	1.596	0.018	1.204	0.010	*
B	550	<i>M. barleaanum</i>	D	1.5–2	1.905	0.021	1.317	0.011	*
K	650	<i>M. barleaanum</i>	D	6–8	2.783	0.031	1.427	0.011	*
A	1000	<i>M. barleaanum</i>	D	3–3.5	2.857	0.031	1.367	0.011	*
C	250	<i>Globobulimina</i> spp.	L	3.5–4	4.169	0.054	2.500	0.025	X
C	250	<i>Globobulimina</i> spp.	L	3.5–4	4.092	0.053	2.557	0.026	X
FP13	375	<i>Globobulimina</i> spp.	L	5–6	4.307	0.056	2.596	0.026	X
B	550	<i>Globobulimina</i> spp.	D	1.5–2	6.842	0.089	2.477	0.025	X
K	650	<i>Globobulimina</i> spp.	D	2–3	3.728	0.048	2.535	0.025	X
K	650	<i>Globobulimina</i> spp.	L	3–4	4.951	0.064	2.602	0.026	X
E	750	<i>Globobulimina</i> spp.	L	2–2.5	3.081	0.040	2.545	0.025	X
A	1000	<i>Globobulimina</i> spp.	L	1–1.5	6.299	0.082	2.498	0.025	X
A	1000	<i>Globobulimina</i> spp.	D	4–5	0.994	0.013	2.007	0.020	X

4.2. Epifaunal Species

The Mg/Ca values for *H. elegans* (Figure 3) range from 0.278 to 1.385 mmol.mol⁻¹ for dead specimens from station WH (1993 m), and from 0.573 to 2.533 mmol.mol⁻¹ for live individuals from stations WH (1993 m) and FP11 (1600 m), respectively.

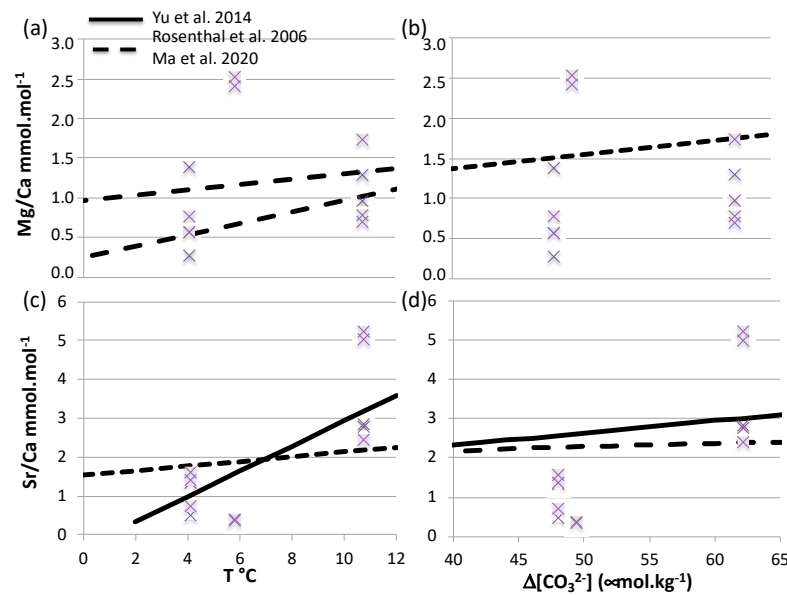


Figure 3. Variations in Mg/Ca (a,b) and Sr/Ca (c,d) versus temperature (a,c) and $\Delta[\text{CO}_3^{2-}]$ (b,d) for *Hoeglundina elegans*. Empty and solid symbols (crosses) represent data obtained on dead and live specimens, respectively. The black curves were obtained on the same species by [51] (solid line) and [50,67] (dotted line).

For the stations where comparison is possible, there are significant differences between the results obtained from dead and live specimens. Furthermore, the values obtained on the same samples by the two instruments show contrasting results, with similar results in some cases (e.g., 1.297 and 1.292 mmol.mol⁻¹ obtained respectively by ICP-OES and ICP-MS-HR for 'dead' *H. elegans* from station B at 2–2.5 cm depth) and different in others (e.g., 2.411 and 1.117 mmol.mol⁻¹ obtained respectively by ICP-OES and ICP-MS-HR for 'live' *H. elegans* from station FP11 at 0–0.5 cm depth). Finally, no clear trend was observed between Mg/Ca and temperature or $\Delta[\text{CO}_3^{2-}]$.

The Sr/Ca of living *H. elegans* specimens is between 0.352 and 5.213 mmol.mol⁻¹ for stations FP11 (1600 m) and B (550 m), respectively, and range from 0.485 (station WH, 1993 m) to 5.165 (station B, 550 m) mmol.mol⁻¹ for dead individuals. The values obtained from dead and living specimens from the same stations also give contrasting results, with identical ratios at some sites (e.g., station WH, same levels) and significantly different ratios at others (e.g., station B, different levels). The values obtained by ICP-OES or ICP-MS-HR are also comparable in some samples (e.g., station WH) but different in other locations (e.g., station B). Finally, the Sr/Ca ratio appears to show higher values as temperature or $\Delta[\text{CO}_3^{2-}]$ increases. The observed variations appear to be in line with the results of [51] for the Sr/Ca-T °C relationship, but are in less agreement with the Sr/Ca- $\Delta[\text{CO}_3^{2-}]$ correlation as defined by [50,67].

The Mg/Ca and Sr/Ca of living *H. balthica* vary respectively from 3.486 and 6.366 (station G, 400 m) and from 1.579 (station G, 400 m) to 3.578 mmol.mol⁻¹ (station B, 550 m) (Figure 2 and Table 3). It is not possible to compare dead and living individuals for this species, and, furthermore, the data obtained are highly variable depending on the instrument used but consistent with each other for each technique. Finally, as the stations where *H. balthica* was found are close, the contrast in temperature and $\Delta[\text{CO}_3^{2-}]$ is not very marked, making it difficult to interpret these data, which is an area for future work. In addition, there is little work on the geochemistry of this species, but previous experience has already demonstrated a high level of intra- and inter-test variability [68].

4.3. Endofaunal Species

Mg/Ca values for *U. peregrina* range from 0.900 to 2.589 mmol.mol⁻¹ for living individuals (stations FP11, 1600 m and G, 400 m, respectively) and are between 0.791 (station WH, 1993 m) and 2.149 (station FP11, 1600 m) mmol.mol⁻¹ for dead specimens (Figure 4a,b). For dead specimens, Sr/Ca results vary from 1.118 (FP11, 1600 m) to 2.646 (station B, 550m); for living individuals, values range from 2.381 (station FP11, 1600 m) to 2.724 (station G, 400 m) mmol.mol⁻¹ (Figure 4c,d). The dead/alive comparison concerns only certain stations, but applies to different levels inside the sediment, as well as the comparison between the two analytical approaches.

The Mg/Ca of 'dead' *U. mediterranea* shows minimum and maximum values of 0.800 and 1.179 mmol.mol⁻¹, respectively, for the same station A (1000 m) (Figure 4a,b). Living specimens exhibit results ranging from 0.776 to 1.319 mmol.mol⁻¹ at station FP12 (800 m) (Figure 4a,b). Sr/Ca results for living specimens range from 1.517 (station B, 550 m) to 2.835 (station A, 1000 m); results range from 1.506 (station A, 1000 m) to 2.594 (station B, 550 m) mmol.mol⁻¹ for dead individuals (Figure 4c,d). The comparison of the values obtained between instruments on the same samples gives contrasting results, sometimes identical (e.g., Mg/Ca from station B) and sometimes variable (e.g., Sr/Ca from station B). The direct comparison between dead and alive must be carefully done since the analyzed levels are close but different.

The calibration curves from the literature obtained for Mg/Ca by [29,31] are consistent with the results obtained (Figure 4a,b) and appear to show a better correlation with temperature. In contrast, the curve of [51] for Sr/Ca is close to the lowest values obtained, which are all associated with ICP-MS-HR measurements (Figure 4c,d) and seem in better agreement with the Sr/Ca- $\Delta[\text{CO}_3^{2-}]$ correlation.

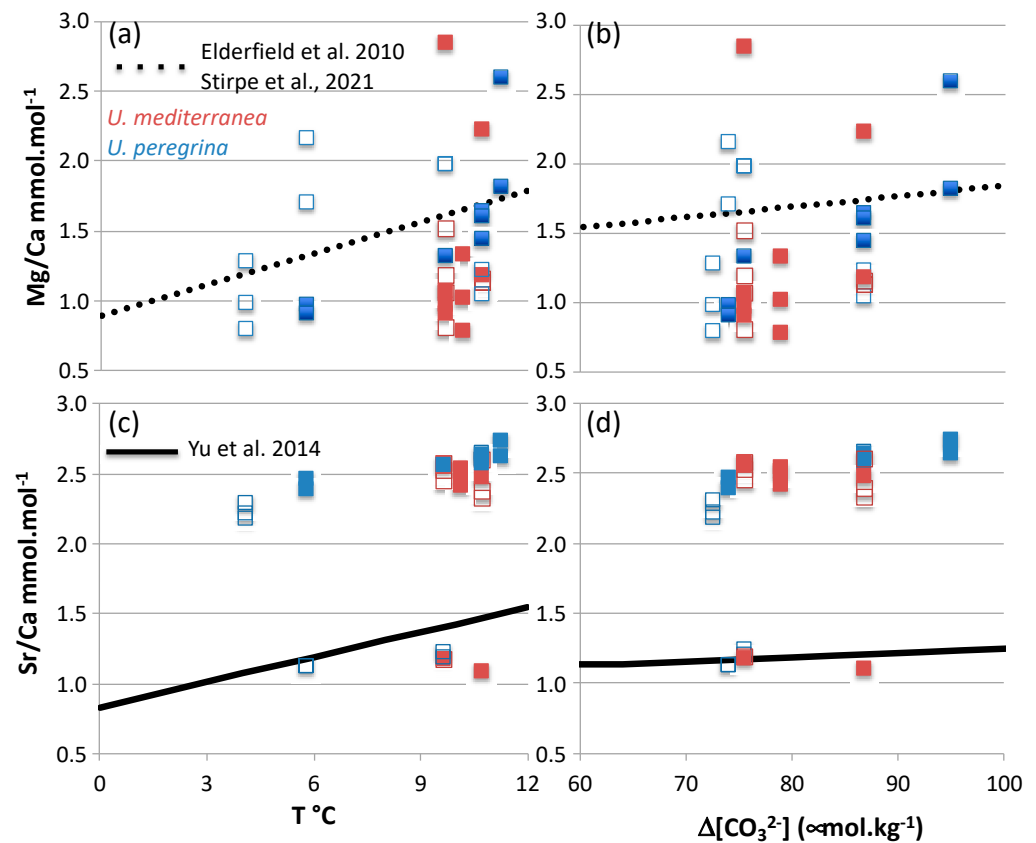


Figure 4. Variations in Mg/Ca (a,b) and Sr/Ca (c,d) versus temperature (a,c) and $\Delta[\text{CO}_3^{2-}]$ (b,d) for *Uvigerina peregrina* (blue) and *Uvigerina mediterranea* (red). Empty and full symbols represent data obtained from dead and live specimens, respectively. The black curves were obtained on *Uvigerina* spp. by [51] (solid line) and [29,31], the two latest calibrations being statistically indistinguishable for temperature (dashed line).

Mg/Ca values range from 1.596 (station FP13, 375 m) to 3.121 (station C, 250 m) mmol.mol^{-1} for live *M. barleeanum*, and from 1.905 (station B, 550 m) to 2.857 (station A, 1000 m) mmol.mol^{-1} for dead specimens (Figure 5a,b). Sr/Ca range from 1.317 (station B, 550 m) to 1.427 (station K, 650 m) mmol.mol^{-1} and from 1.204 (station FP13, 375 m) to 1.327 (station C, 250 m) mmol.mol^{-1} for dead and living individuals, respectively (Figure 5c,d).

Results for living *Globobulimina* spp. specimens range from 3.081 (station E, 750 m) to 6.299 (station A, 1000 m) mmol.mol^{-1} and from 2.448 (station A, 1000 m) to 2.602 (station K, 650 m) mmol.mol^{-1} for the Mg/Ca and the Sr/Ca ratios, respectively (Figure 5). For dead individuals, minimum and maximum Mg/Ca values are 0.994 (station A, 1000 m) and 6.842 (station B, 550 m) mmol.mol^{-1} , respectively. Results for Sr/Ca range from 2.007 (station A, 1000 m) to 2.535 (station K, 650 m) mmol.mol^{-1} (Figure 5).

Comparison of the data obtained with the literature shows a good agreement between the Mg/Ca of *M. barleeanum* and the curves of [69,70], as well as between the Mg/Ca of *Globobulimina* spp. and the work of [71] (Figure 5a). Nevertheless, the range of variation in the values obtained remains low, particularly for Sr/Ca, which appears to correlate little with temperature or $\Delta[\text{CO}_3^{2-}]$. Specimens of *M. barleeanum* and *Globobulimina* spp. were all analyzed by ICP-MS-HR or ICP-OES respectively, which does not allow inter-instrument comparison. Comparisons between dead and living individuals are scarce because the samples come from different stations or from different levels within the same station.

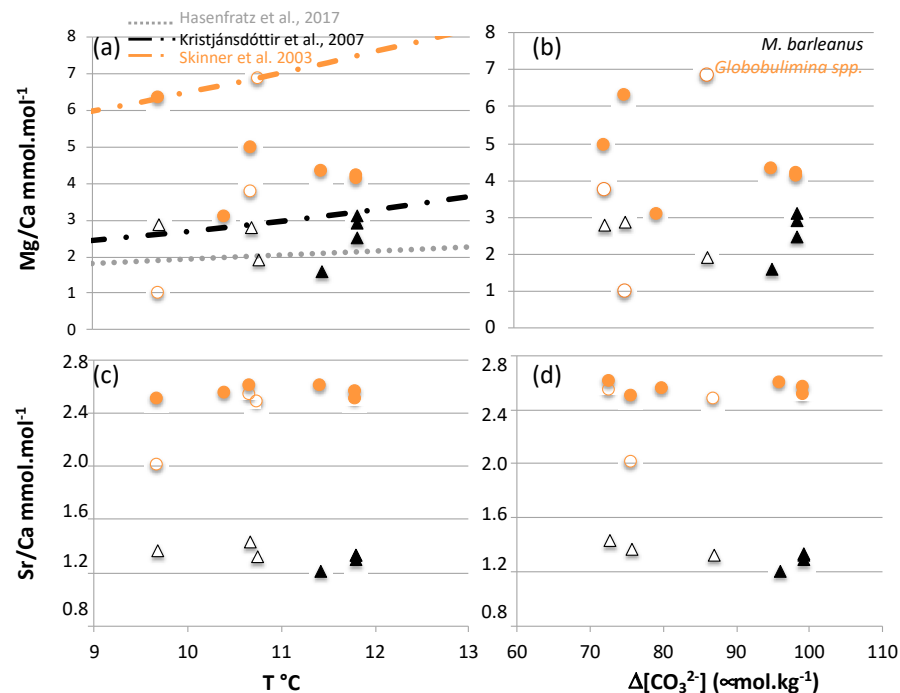


Figure 5. Variations in Mg/Ca (a,b) and Sr/Ca (c,d) versus temperature (a,c) and $\Delta[\text{CO}_3^{2-}]$ (b,d) for *Melonis barleeanum* (black) and *Globobulimina* spp. (orange). Empty and solid symbols represent data obtained from dead and live specimens respectively. The dotted black and grey curves were obtained on *Melonis barleeanum* by [69,70], respectively, and the orange curve on *Globobulimina affinis* by [71].

5. Discussion

5.1. Results of Living versus Dead Specimens

The direct comparison between results from live and dead specimens is limited to species for which both kinds of specimens were available. They comprise the following:

- *H. elegans* at stations B (550 m) and WH (1993 m);
- *U. mediterranea* at stations B (550 m) and A (1000 m);
- *U. peregrina* at stations B (550 m), A (1000 m), and FP11 (1600 m);
- *Globobulimina* spp. at stations K (650 m) and A (1000 m).

Moreover, some results that are compared strictly come from the same depth but in some cases, the depth was close but not identical (see Table 3 for details).

When comparing values of Mg/Ca of *H. elegans* between dead and live specimens (Figure 6, Panel A(a–d)), we observe similar average values of $1.186 (\pm 0.188, 1\sigma)$ and $1.298 (\pm 0.968, 1\sigma)$ mmol.mol^{-1} , respectively, considering the high dispersion of the data (especially from live *H. elegans*) at station B (Figure 6, Panel A(a,b)). At station WH (Figure 6, Panel A(c,d)), the Mg/Ca values of ‘dead’ specimens are more variable than for the ‘living’ ones, with average values of $0.831 (\pm 0.783, 1\sigma)$ and $0.686 (\pm 0.102, 1\sigma)$, respectively. It seems that one value of Mg/Ca of living *H. elegans* ($2.416 \text{ mmol.mol}^{-1}$, station B) is out of the expected range of values for this species. This could be attributed to: (i) the difference in the depth of retrieval of the sample (0.5–1 cm, the shallowest sample of all of them) or (ii) the difference in the analytical procedure (measurement by ICP-MS), this latter point being recently discussed in the literature. However, when removing this value, the difference between the Mg/Ca of dead and living *H. elegans* increases and becomes statistically significant (average of $0.740 \pm 0.005, 1\sigma$). Average values of Sr/Ca (Figure 6, Panel A(e–h)) of ‘living’ *H. elegans* are $3.986 (\pm 1.947, 1\sigma)$ mmol.mol^{-1} , close to the results from ‘dead’ specimens at $3.588 (\pm 1.366, 1\sigma)$ mmol.mol^{-1} . At station WH (Figure 6, Panel A(g–h)), the average Sr/Ca is $1.182 (\pm 0.535, 1\sigma)$ and $0.912 (\pm 0.603, 1\sigma)$ mmol.mol^{-1} for

‘living’ and ‘dead’ *H. elegans*, respectively. However, as observed for the Mg/Ca data, the dispersion is high, especially when looking at the instrument used for analysis.

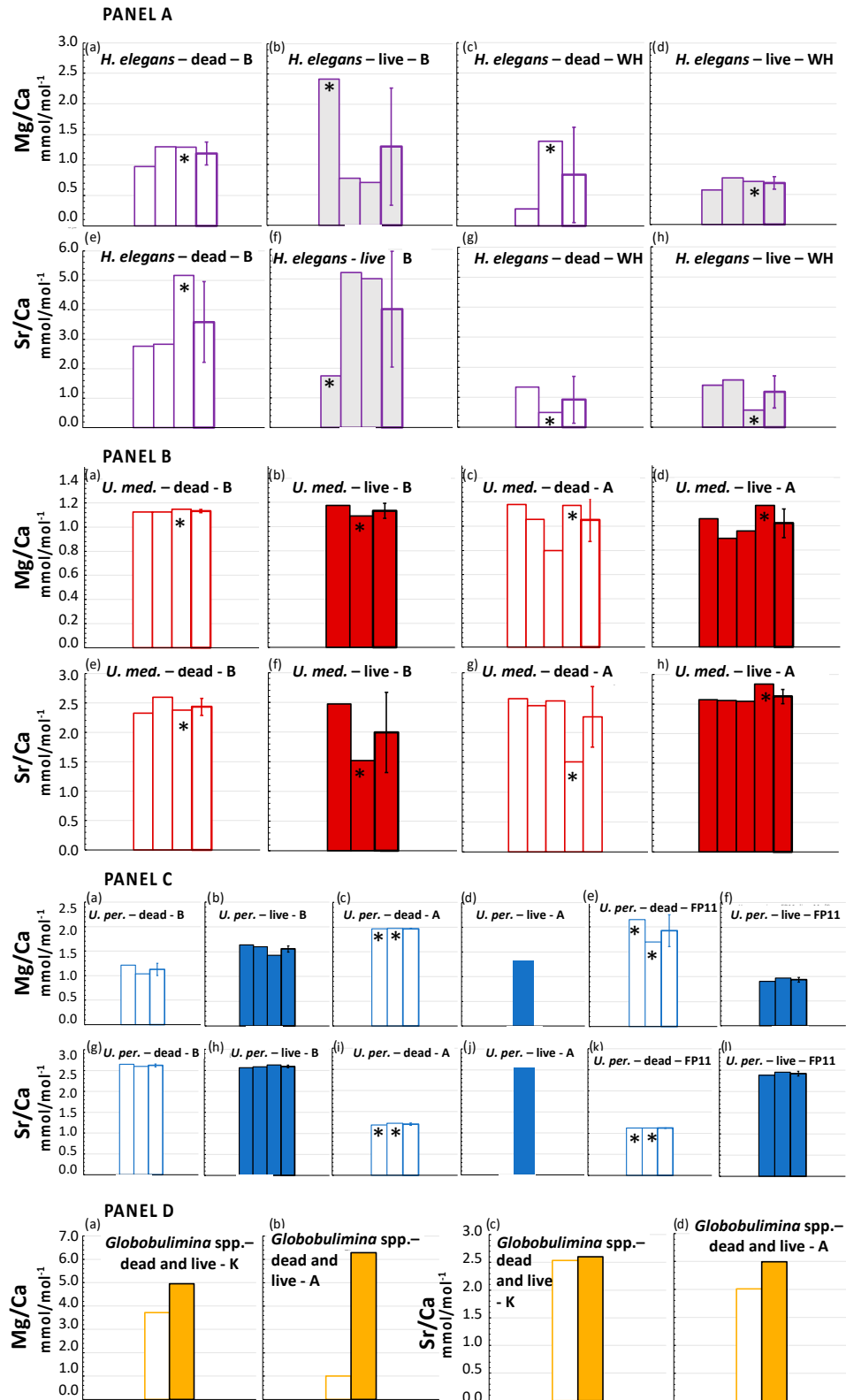


Figure 6. Comparison between results from dead and live specimens (empty and full bar, respectively). The average values are reported as the last bar with bold contour, error is given as 1σ . Asterisks indicate results obtained by ICP-MS, the other data being measured by ICP-OES. [Panel A: Purple:

Hoeglundina elegans; (a–d): Mg/Ca; (e–h): Sr/Ca; (a,b,e,f): station B; (c,d,g,h): station WH.]; [Panel B: Red: *U. med.* for *Uvigerina mediterranea*; (a–d): Mg/Ca; (e–h): Sr/Ca; (a,b,e,f): station B; (c,d,g,h): station A.]; [Panel C: Blue: *U. per.* for *Uvigerina peregrina*; (a–f): Mg/Ca; (g–l): Sr/Ca; (a,b,g,h): station B; (c,d,i,j): station A; (e,f,k,l): station FP11.]; [Panel D: Orange: *Globobulimina* spp.; (a,b): Mg/Ca; (c,d): Sr/Ca; (a,c): station K; (b,d): station A].

U. mediterranea average results of Mg/Ca measured in dead specimens (Figure 6, Panel B(a–c)) are $1.134 (\pm 0.013, 1\sigma)$ and $1.052 (\pm 0.177, 1\sigma)$ mmol.mol⁻¹ at stations B and A, respectively, statistically equivalent to values $1.131 (\pm 0.006, 1\sigma)$ and $1.022 (\pm 0.119, 1\sigma)$ mmol.mol⁻¹ obtained from living specimens (Figure 6, Panel B(b,d)) from the same stations. Average values of Sr/Ca at stations B (Figure 6, Panel B(e,f)) and A (Figure 6, Panel B(g,h)) are $1.995 (\pm 0.675, 1\sigma)$ and $2.628 (\pm 0.139, 1\sigma)$ mmol.mol⁻¹, and $2.431 (\pm 0.143, 1\sigma)$ and $2.260 (\pm 0.505, 1\sigma)$ for living and dead specimens, respectively. Overall, values of *U. mediterranea* are poorly scattered at one station and exhibit a good agreement between live and dead specimens.

For *U. peregrina*, the comparison can be done for three stations but we only measured one living specimen at station A. Moreover, it is important to notice that all living specimens were measured by ICP-OES whereas some analyses were performed by ICP-MS for dead specimens (stations A and FP11). Mg/Ca values for dead specimens (Figure 6, Panel C(a,c,e)) are $1.128 (\pm 0.125, 1\sigma)$, $1.968 (\pm 0.003, 1\sigma)$, and $1.925 (\pm 0.317, 1\sigma)$ mmol.mol⁻¹ at stations B, A, and FP11, respectively. Values obtained from living specimens are statistically different, higher at station B ($1.155 \text{ mmol.mol}^{-1} \pm 0.111, 1\sigma$, Figure 6, Panel C(b)) and lower at stations A ($1.317 \text{ mmol.mol}^{-1}$, Figure 6, Panel C(d)) and FP11 ($0.934 \text{ mmol.mol}^{-1} \pm 0.048, 1\sigma$, Figure 6, Panel C(f)). Sr/Ca results are similar between dead ($2.619 \text{ mmol.mol}^{-1} \pm 0.037, 1\sigma$) and live ($2.594 \text{ mmol.mol}^{-1} \pm 0.034, 1\sigma$) specimens from station B (Figure 6, Panel C(g,h)). However, there was a significant difference at station A (Figure 6, Panel C(i,j)), with higher values for living specimens ($2.557 \text{ mmol.mol}^{-1}$) compared to dead specimens ($1.203 \text{ mmol.mol}^{-1} \pm 0.026, 1\sigma$), and the opposite trend for station FP11 ($2.418 \text{ mmol.mol}^{-1} \pm 0.053, 1\sigma$, versus $1.119 \text{ mmol.mol}^{-1} \pm 0.002, 1\sigma$, respectively, Figure 6, Panel C(k,l)).

Overall values are lower for dead specimens of *Globobulimina* spp. for Mg/Ca and Sr/Ca at stations K and A when the comparison was possible, but analysis was only performed on one sample each time: 3.728 versus $4.951 \text{ mmol.mol}^{-1}$ and 0.994 versus $6.299 \text{ mmol.mol}^{-1}$ for ‘dead’ and ‘live’ Mg/Ca at stations B and K, respectively, and 2.535 versus $2.602 \text{ mmol.mol}^{-1}$ and 2.007 versus $2.498 \text{ mmol.mol}^{-1}$ for ‘dead’ and ‘live’ Sr/Ca at stations B and K, respectively. However, it seems that Sr/Ca values are in better agreement between ‘dead’ and ‘living’ specimens than the Mg/Ca results were.

Finally, there is no clear trend when comparing dead and live specimens’ values, as the dispersion of the values can be high in both sets of samples. Moreover, as measurements have been performed on different instruments, and at different depths inside the sediment, there may be additional processes that could influence the geochemical signature.

However, results from the *Uvigerina* genus seem to be less scattered and in better agreement between ‘live’ and ‘dead’ specimens than for other species. An increase in the number of data in the future would be crucial to improve the statistical significance of these differences.

5.2. Comparison between Analytical Approaches

The comparison between values obtained from the two instruments gives contrasting results.

Indeed, the Mg/Ca of dead *H. elegans* measured by both ICP-OES and ICP-MS are in good agreement at station B (Figure 6, Panel A(a)) whereas values are significantly different at station WH (Figure 6, Panel A(c)); the opposite trend is observed for living specimens, with values in good agreement at station WH (Figure 6, Panel A(d)) but different at station B (Figure 6, Panel A(b)). The Sr/Ca ratios measured by both techniques are always different

in any case (Figure 6, Panel A(e–h)). At station FP11, both the Mg/Ca and the Sr/Ca of living *H. elegans* are significantly different depending on the instrument (Figure 7a–d).

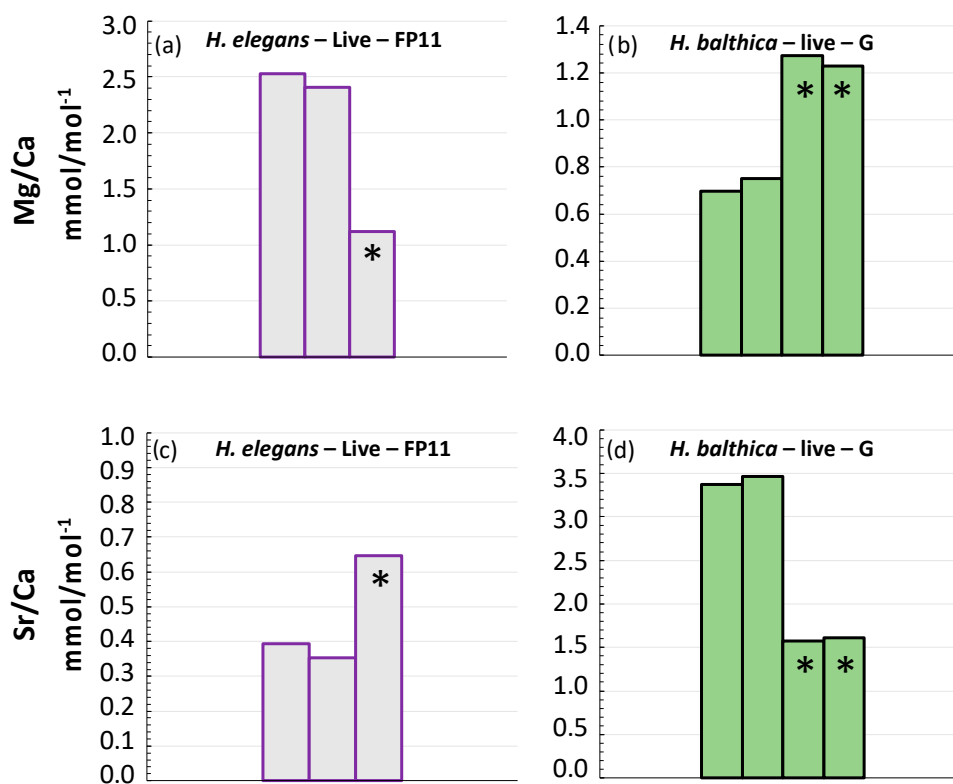


Figure 7. Comparison between results of living specimens from the same station measured by ICP-OES and ICP-MS (asterisks). (a,c) Purple: living *Hoeglundina elegans* from station FP11; (a) Mg/Ca; (c) Sr/Ca. (b,d) Green: living *Hyalinea balthica* from station G; (b) Mg/Ca; (d) Sr/Ca.

For *U. mediterranea*, values are in good agreement for the Mg/Ca from living or dead specimens at all stations (Figure 6, Panel B(a–d)). There is no global trend for Sr/Ca values, which are in good agreement for living and dead specimens for stations B (Figure 6, Panel B(e)) and A (Figure 6, Panel B(h)), respectively, but significantly different for living specimens at station B (Figure 6, Panel B(f)) and dead ones at station A (Figure 6, Panel B(g)).

The Mg/Ca (Figure 7b) and the Sr/Ca (Figure 7d) of *H. balthica* are in good agreement for each instrument but significantly different between both techniques.

There is no special trend in the observed difference, i.e., values can be both higher or lower on both instruments, and there is no trend between the Mg/Ca and the Sr/Ca from the same sample, i.e., Mg/Ca values can be higher (or lower) and Sr/Ca lower (or higher).

We calculated the external reproducibility for each instrument, i.e., when replicates of strictly the same sample were measured (Table 4). The external reproducibility for Mg/Ca ranges from 0.1 to 26%, with an average of about 12% ($n = 15$), and from 0.2 to 17%, with an average of 7.5% ($n = 4$), for ICP-OES and ICP-MS, respectively. For Sr/Ca, the external reproducibility is between 0.5 and 8.7% (average of 3.2%, $n = 15$) and 0.1 to 2.2% (average of 1.4%, $n = 4$) for ICP-OES and ICP-MS, respectively. Thus, the analytical conditions are close between both instruments (despite fewer measurements on the ICP-MS compared to the ICP-OES). There is no special trend between living and dead specimens' measurements.

The analysis of our results does not allow us to decipher a special trend. Differences between technical approaches have already been observed [72], for instance between LA-ICP-MS and ICP-MS [31]. A strong dispersion of the data is especially measured by LA-ICP-MS [31,48,73] or by SIMS [73], reflecting the intra-test variability. This could be

related to biomineralization processes, since in this study, we worked in conditions where the impact of early diagenesis should be limited.

Table 4. External reproducibility of replicate measurements by ICP-OES (X) and ICP-MS (*). The letters “L” and “D” refer to live and dead specimens, respectively.

Station	Water Depth (m)	Species	D/L	Depth inside the Sediment (cm)	Average Mg/Ca (mmol.mol ⁻¹)	1 s	Mg/Ca External Reproducibility	Average Sr/Ca (mmol.mol ⁻¹)	1 s	Sr/Ca External Reproducibility	n=	Instrument
B	550	<i>H. elegans</i>	L	1–1.5	0.740	0.054	7.3%	5.109	0.147	2.9%	2	X
B	550	<i>H. elegans</i>	D	2–2.5	1.133	0.232	21%	2.799	0.050	1.8%	2	X
FP11	1600	<i>H. elegans</i>	L	0–0.5	2.472	0.087	3.5%	0.373	0.029	7.9%	2	X
WH	1993	<i>H. elegans</i>	L	0–0.5	0.672	0.140	21%	1.486	0.130	8.7%	2	X
G	400	<i>H. balthica</i>	L	0–0.5	3.621	0.191	5.3%	3.419	0.059	1.7%	2	X
G	400	<i>H. balthica</i>	L	0–0.5	6.255	0.157	2.5%	1.593	0.020	1.2%	2	*
B	550	<i>H. balthica</i>	L	1–1.5	3.805	0.317	8.3%	3.533	0.063	1.8%	2	X
B	550	<i>U. mediterranea</i>	D	1–1.5	1.127	0.001	0.1%	5.459	0.191	7.8%	2	X
FP12	800	<i>U. mediterranea</i>	L	0–0.5	1.037	0.272	26%	2.483	0.065	2.6%	3	X
A	1000	<i>U. mediterranea</i>	L	0–0.5	0.972	0.081	8.3%	2.558	0.013	0.5%	3	X
A	1000	<i>U. mediterranea</i>	D	1–1.5	1.011	0.193	19%	2.511	0.060	2.4%	3	X
G	400	<i>U. peregrina</i>	L	0–0.5	2.198	0.552	25%	2.674	0.071	2.7%	2	X
B	550	<i>U. peregrina</i>	L	0–0.5	1.618	0.029	1.8%	2.576	0.018	0.7%	2	X
A	1000	<i>U. peregrina</i>	D	5.5–6.5	1.968	0.003	0.2%	1.203	0.026	2.2%	2	*
FP11	1600	<i>U. peregrina</i>	L	1–1.5	0.934	0.048	5.2%	2.418	0.053	2.2%	2	X
FP11	1600	<i>U. peregrina</i>	D	3–3.5	1.925	0.317	17%	1.119	0.002	0.1%	2	*
WH	1993	<i>U. peregrina</i>	D	0–0.5	1.012	0.242	24%	2.222	0.062	2.8%	3	X
C	250	<i>M. barleanus</i>	L	5–6	2.695	0.294	11%	1.310	0.025	1.9%	2	*
C	250	<i>Globobulimina</i> spp.	L	3.5–4	4.130	0.054	1.3%	2.528	0.040	1.6%	2	X

However, we could perhaps discuss the efficiency of the cleaning procedure. Indeed, in this work we chose to apply the sample preparation from [43] that does not include the reductive step from the original protocol of [74]. This approach could be insufficiently efficient to ensure reproducibility between living and dead foraminifera, between stations, or between instruments. However, even if we apply the correction of minus 0.2 mmol.mol⁻¹ that has been applied between both procedures [29], this will not resolve the difference and the variability observed in our results. As the calculated external reproducibility is higher for Mg/Ca than for Sr/Ca, the Mg/Ca ratio seems to be more sensitive to analytical conditions or sample preparation, as already demonstrated in laboratory studies [44]. Previous works [75–77] have also used an extended version of the oxidative step (50% buffered H₂O₂ for 45 min) of the short protocol from [43], as a precaution to eliminate the potential higher organic matter contents found in core top material. We suggest that the systematic use of the full cleaning method should be chosen to avoid problems associated with technical conditions; however, this will not solve the natural intra-test or inter-test variability (see also Section 5.3.2). In this context, some species seem to be better candidates for palaeoceanographic reconstructions.

5.3. Choice of Species for Paleoceanographic Reconstructions

5.3.1. Towards a Global Calibration Dataset?

As we worked on six different species, we can discuss their respective potential for palaeoceanographic reconstructions. However, in our study, the temperature and Δ[CO₃²⁻] ranges of variations remain low, as the studied stations are close geographically and in depth (Figure 1 and Table 1). The best approach is thus to combine the obtained dataset with previous works, in order to refine the existing calibrations. We already compared our results with previous calibrations for each species and demonstrated that they are

in good agreement with the literature (see Section 4, Figures 3–5). As the relationship between Mg/Ca and temperature is well-documented in the literature, we plotted the obtained data from all species (except *H. elegans* because the aragonitic nature of the test induced a geochemical behavior different than calcitic species), together with published calibrations of *Globobulimina* spp. [71], *Cibicidoides* spp. and *Oridorsalis umbonatus* [32], *M. barleeaanum* [69,70], *Uvigerina* spp. [29,31], as well as the relationship obtained with inorganic calcite [7] (Figure 8). The overall dataset fits well with the published calibrations, and, except for *Globobulimina* spp. and *H. balthica* with higher values than the other species, the variability of the results falls within the limits defined by the existing relationships. Thus, the only way to increase the robustness of the environmental reconstructions is to provide more data in the future, allowing an increase in the precision and sensitivity of a proxy to a given environmental parameter. However, to decipher the different sources of influence on a proxy, several parameters must be tested.

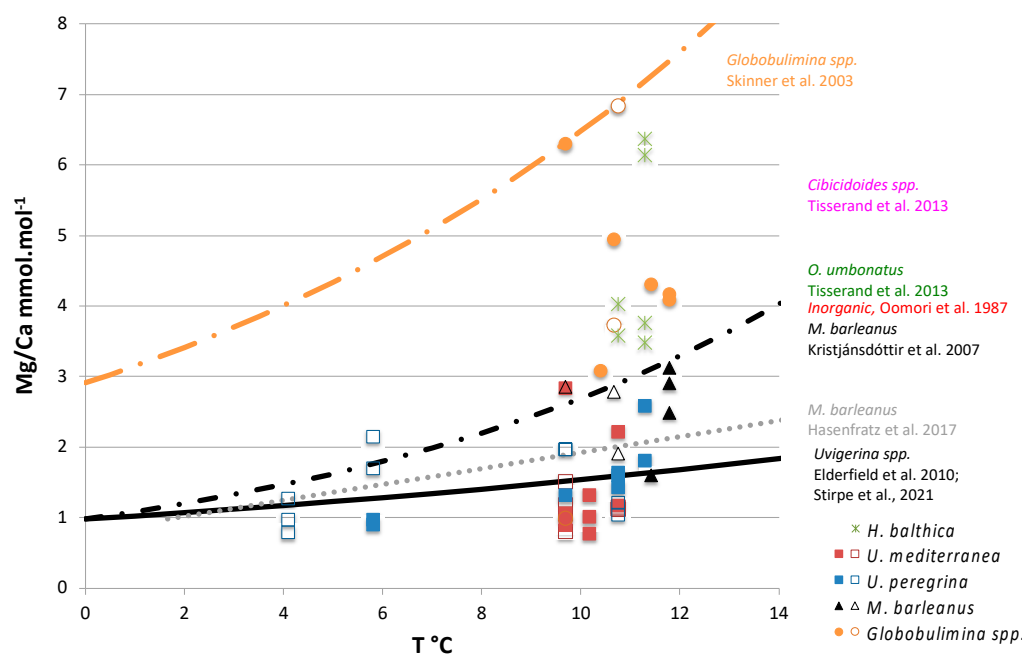


Figure 8. Compilation of published data on the relationship between Mg/Ca and temperature for the studied calcitic species and other species: orange line and circles: *Globobulimina* spp. [71]; pink line: *Cibicidoides* spp. and green line: *Oridorsalis umbonatus* [32]; *Melonis barleeaanum*: black dotted line and triangles [69] and grey dotted line [70]; *Uvigerina* spp.: red and blue squares, and bold black line [29,31]. The calibration obtained by precipitation of inorganic calcite is also reported in light red [7]. Empty and full symbols represent data obtained from dead and live specimens, respectively.

5.3.2. *U. mediterranea* vs. *U. peregrina*

In the following, we chose to discuss in detail the species of the *Uvigerina* genus. Indeed, our dataset tends to show that *U. mediterranea* and *U. peregrina* are the best candidates to obtain robust calibrations, since the differences between living and dead specimens and the external reproducibility are the lowest observed (Figure 6, Panel B,C and Table 4). To better analyze our results, we plotted the average values with their external reproducibilities (Table 4) together with the full dataset (Figure 9).

Values of Mg/Ca (Figure 9a,b) and Sr/Ca (Figure 9c,d) of *U. mediterranea* and *U. peregrina* are significantly different, meaning that the mixing between different species of the *Uvigerina* genus can be questioned, although it has been done already in previous works to provide global calibrations [26,28–30,78]. Moreover, in our study, values of *U. mediterranea* do not exhibit a strong variability throughout the environmental conditions, whereas the Mg/Ca and Sr/Ca values of *U. peregrina* change with temperature and $\Delta[\text{CO}_3^{2-}]$ (Figure 9).

The Sr/Ca values of both species are scattered and do not cover a large range of values (Figure 8c,d). An explanation for this variability could be related to the microhabitat of the *Uvigerina* species. Indeed, we measured specimens coming from different depths inside the sediment (Table 3), that live in various geochemical compositions of the surrounding porewater. Thus, our data tend to show that the Sr/Ca ratio may be more influenced by the living depth inside the sediment, as already suggested [31] for the Mg/Ca of *U. peregrina*. From a broader perspective, the significance of the Sr/Ca ratio is not fully understood, depending on species and locations, even though more and more studies point towards a control of the C-system such as the $\Delta[\text{CO}_3^{2-}]$ [48,50,51,73].

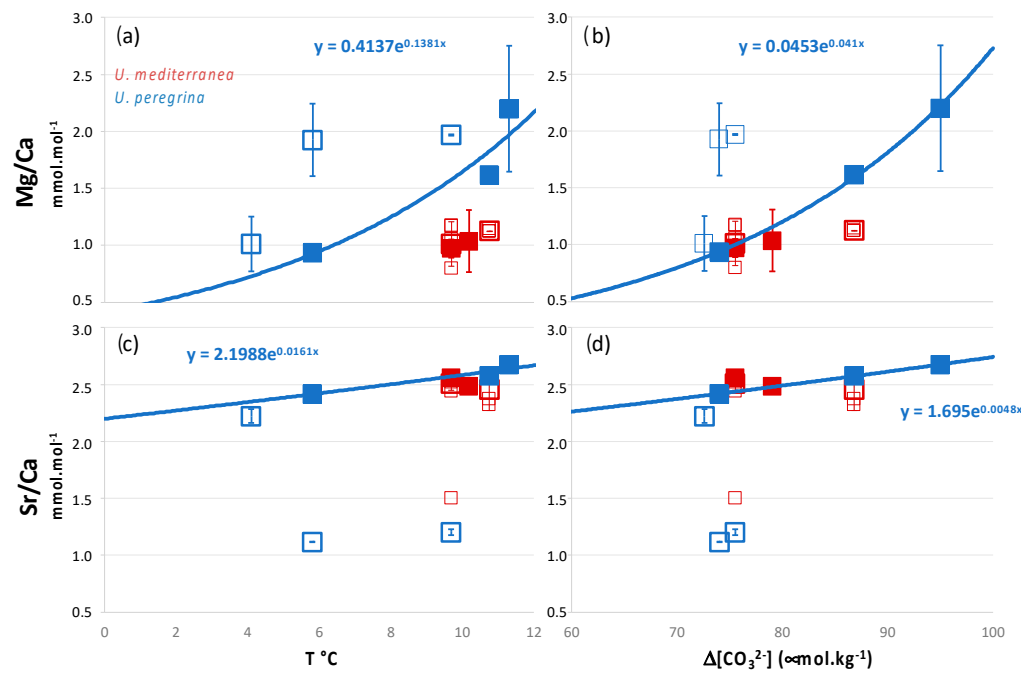


Figure 9. Variations in Mg/Ca (a,b) and Sr/Ca (c,d) versus temperature (a,c) and $\Delta[\text{CO}_3^{2-}]$ (b,d) for *Uvigerina peregrina* (blue) and *Uvigerina mediterranea* (red). Empty and full symbols represent data obtained from dead and live specimens, respectively. The average values are indicated with larger symbols with error bars corresponding to the external reproducibility (Table 4). The blue curve corresponds to the calculated correlation including only the data measured in living specimens of *U. peregrina* (see text for explanation).

We chose to explore the correlation between the temperature and $\Delta[\text{CO}_3^{2-}]$ and the average Mg/Ca values of living specimens of *U. peregrina* (Figure 8a,b). Indeed, this is the most complete dataset measured with one unique instrument (ICP-OES), allowing us to avoid variability due to technical approaches (Tables 3 and 4). We assume that drawing a correlation using only a few points must be cautiously considered, and this is the reason why we do not provide the coefficient correlation, because in this context, it may not be statistically robust. However, the interesting observation is that within our dataset, there is no better correlation between the Mg/Ca and the temperature (Figure 8a) or $\Delta[\text{CO}_3^{2-}]$ (Figure 8b). The influence of $\Delta[\text{CO}_3^{2-}]$ has already been discussed for *Uvigerina* species [28,29] but there is an admitted assumption that the Mg/Ca of *U. peregrina* is more controlled by temperature than by the $\Delta[\text{CO}_3^{2-}]$. Indeed, infaunal species such as the *Uvigerina* genus are supposed to live inside the sediment, where the $\Delta[\text{CO}_3^{2-}]$ reaches 0 and below in the first centimeters of depth [79,80], buffering the impact of changes in the $\Delta[\text{CO}_3^{2-}]$ of bottom-waters. Our observations need to be confirmed with more data, but this assumption may not be valid in all ocean contexts, and should be better documented. Moreover, there are few data about the $\Delta[\text{CO}_3^{2-}]$ of porewater, and more investigations could help to explain this point. A complementary approach could also be the analysis of

the individual and even of the intra-test variability by LA-ICP-MS or SIMS, for instance (e.g., [48,68]).

6. Conclusions

In order to better constrain the relationships between the Mg/Ca and Sr/Ca ratio with environmental parameters, we performed elemental analysis on six different species of benthic foraminifera (*Hoeglundina elegans* and *Hyalinea balthica* from the epifauna, *Uvigerina peregrina*, *U. mediterranea* and *Melonis barleeanum* from the superficial to intermediate endofauna, and *Globobulimina* spp. from the deep endofauna) from the Bay of Biscay with two different analytical approaches (ICP-OES and ICP-MS). Our results are in overall good agreement with previous studies, fitting well with published calibrations. However, we point out a strong variability in the results: (i) between living and dead specimens; (ii) between both instrumental approaches. We discussed the impact of the cleaning procedure, as well as the natural variability between samples from the same station coming from different depths inside the sediment, even when they are close together. Finally, we focus on species from the *Uvigerina* genus (*U. peregrina* and *U. mediterranea*) since they present the most reduced external reproducibility and the best agreement between living and dead specimens. Our results show that the two species should not be mixed for analysis, with lower values and a reduced range of variability for *U. mediterranea* compared to *U. peregrina*. In our dataset, the control of the temperature on the Mg/Ca ratio of *U. peregrina* is as strong as the $\Delta[\text{CO}_3^{2-}]$, suggesting a need to consider BWT reconstructions when not considering the potential impact of the $\Delta[\text{CO}_3^{2-}]$.

Author Contributions: Conceptualization, S.S., M.M., F.B. and J.B.; Methodology, S.S., M.T., M.M., F.B., M.-P.N., P.-A.D. and J.B.; Formal analysis, S.S., M.T., M.M., F.B., M.-P.N. and J.B.; Writing—original draft preparation, S.S.; Writing—review and editing, S.S., M.T., F.B., M.M., M.-P.N., P.-A.D. and J.B.; Funding acquisition, S.S. All authors have read and agreed to the published version of the manuscript.

Funding: This research has been supported by the CNRS (INSU-LEFE-CYBER: Project GeoFoBe).

Institutional Review Board Statement: Not applicable.

Informed Consent Statement: Not applicable.

Data Availability Statement: Data is contained within the article.

Conflicts of Interest: The authors declare no conflicts of interest.

Appendix A

Table A1. Results of Fe/Ca carried out by ICP-OES (X) and ICP-MS-HR (*) on live (L) and dead (D) benthic foraminifera in the Bay of Biscay. See reference for stations in Table 1, and their location in Figure 1a. The Fe/Ca ratio is used as a screening criterion for the efficiency of the cleaning procedure, with a critical value of $<0.1 \text{ mmol}\cdot\text{mol}^{-1}$. n.d.: not determined, i.e., below the limit of quantification.

Station	Water Depth (m)	Species	D/L	Depth inside the Sediment (cm)	Fe/Ca	1 s	Instrument
B	550	<i>H. elegans</i>	L	0.5–1	n.d.	n.d.	*
B	550	<i>H. elegans</i>	L	1–1.5	0.036	0.003	X
B	550	<i>H. elegans</i>	L	1.5–2	0.032	0.002	X
B	550	<i>H. elegans</i>	D	2–2.5	n.d.	n.d.	X
B	550	<i>H. elegans</i>	D	2–2.5	n.d.	n.d.	X
B	550	<i>H. elegans</i>	D	2–2.5	0.101	0.001	*
FP11	1600	<i>H. elegans</i>	L	0–0.5	n.d.	n.d.	X
FP11	1600	<i>H. elegans</i>	L	0–0.5	n.d.	n.d.	X
FP11	1600	<i>H. elegans</i>	L	0–0.5	n.d.	n.d.	*
WH	1993	<i>H. elegans</i>	L	0–0.5	0.069	0.005	X

Table A1. Cont.

Station	Water Depth (m)	Species	D/L	Depth inside the Sediment (cm)	Fe/Ca	1 s	Instrument
WH	1993	<i>H. elegans</i>	L	0–0.5	0.103	0.007	X
WH	1993	<i>H. elegans</i>	D	0–0.5	n.d.	n.d.	X
WH	1993	<i>H. elegans</i>	D	0–0.5	n.d.	n.d.	*
WH	1993	<i>H. elegans</i>	L	0.5–1	n.d.	n.d.	*
G	400	<i>H. balthica</i>	L	0–0.5	n.d.	n.d.	X
G	400	<i>H. balthica</i>	L	0–0.5	n.d.	n.d.	X
G	400	<i>H. balthica</i>	L	0–0.5	0.098	0.001	*
G	400	<i>H. balthica</i>	L	0–0.5	0.082	0.001	*
B	550	<i>H. balthica</i>	L	1–1.5	0.102	0.007	X
B	550	<i>H. balthica</i>	L	1–1.5	0.101	0.007	X
B	550	<i>U. mediterranea</i>	L	0–0.5	n.d.	n.d.	X
B	550	<i>U. mediterranea</i>	L	0–0.5	n.d.	n.d.	*
B	550	<i>U. mediterranea</i>	D	1–1.5	0.063	0.005	X
B	550	<i>U. mediterranea</i>	D	1–1.5	0.042	0.003	X
B	550	<i>U. mediterranea</i>	D	1.5–2	n.d.	n.d.	*
FP12	800	<i>U. mediterranea</i>	L	0–0.5	n.d.	n.d.	X
FP12	800	<i>U. mediterranea</i>	L	0–0.5	n.d.	n.d.	X
FP12	800	<i>U. mediterranea</i>	L	0–0.5	n.d.	n.d.	X
A	1000	<i>U. mediterranea</i>	L	0–0.5	0.030	0.002	X
A	1000	<i>U. mediterranea</i>	L	0–0.5	0.107	0.008	X
A	1000	<i>U. mediterranea</i>	L	0–0.5	0.083	0.006	X
A	1000	<i>U. mediterranea</i>	L	0.5–1	n.d.	n.d.	*
A	1000	<i>U. mediterranea</i>	D	1–1.5	0.031	0.002	X
A	1000	<i>U. mediterranea</i>	D	1–1.5	0.085	0.006	X
A	1000	<i>U. mediterranea</i>	D	1–1.5	0.087	0.006	X
A	1000	<i>U. mediterranea</i>	D	1–1.5	n.d.	n.d.	*
G	400	<i>U. peregrina</i>	L	0–0.5	0.101	0.007	X
G	400	<i>U. peregrina</i>	L	0–0.5	0.046	0.003	X
B	550	<i>U. peregrina</i>	L	0–0.5	0.109	0.008	X
B	550	<i>U. peregrina</i>	L	0.5–1	0.105	0.008	X
B	550	<i>U. peregrina</i>	D	0.5–1	0.113	0.008	X
B	550	<i>U. peregrina</i>	L	1–1.5	0.104	0.007	X
B	550	<i>U. peregrina</i>	D	1–1.5	0.084	0.006	X
A	1000	<i>U. peregrina</i>	L	0–0.5	0.053	0.004	X
A	1000	<i>U. peregrina</i>	D	5.5–6.5	0.066	0.001	*
A	1000	<i>U. peregrina</i>	D	5.5–6.5	0.100	0.001	*
FP11	1600	<i>U. peregrina</i>	L	1–1.5	0.041	0.003	X
FP11	1600	<i>U. peregrina</i>	L	1–1.5	0.044	0.001	X
FP11	1600	<i>U. peregrina</i>	D	3–3.5	0.015	0.001	*
FP11	1600	<i>U. peregrina</i>	D	3–3.5	n.d.	n.d.	*
WH	1993	<i>U. peregrina</i>	D	0–0.5	0.107	0.008	X
WH	1993	<i>U. peregrina</i>	D	0–0.5	0.093	0.007	X
WH	1993	<i>U. peregrina</i>	D	0–0.5	0.034	0.002	X
C	250	<i>M. barleanus</i>	L	0.5–1	0.100	0.001	*
C	250	<i>M. barleanus</i>	L	5–6	0.095	0.002	*

Table A1. Cont.

Station	Water Depth (m)	Species	D/L	Depth inside the Sediment (cm)	Fe/Ca	1 s	Instrument
C	250	<i>M. barleanus</i>	L	5–6	0.099	0.001	*
FP13	375	<i>M. barleanus</i>	L	1–1.5	n.d.	n.d.	*
B	550	<i>M. barleanus</i>	D	1.5–2	0.101	0.001	*
K	650	<i>M. barleanus</i>	D	6–8	0.092	0.001	*
A	1000	<i>M. barleanus</i>	D	3–3.5	0.101	0.001	*
C	250	<i>Globobulimina</i> spp.	L	3.5–4	0.104	0.008	X
C	250	<i>Globobulimina</i> spp.	L	3.5–4	0.066	0.005	X
FP13	375	<i>Globobulimina</i> spp.	L	5–6	0.105	0.008	X
B	550	<i>Globobulimina</i> spp.	D	1.5–2	0.036	0.003	X
K	650	<i>Globobulimina</i> spp.	D	2–3	0.029	0.002	X
K	650	<i>Globobulimina</i> spp.	L	3–4	0.066	0.005	X
E	750	<i>Globobulimina</i> spp.	L	2–2.5	0.103	0.009	X
A	1000	<i>Globobulimina</i> spp.	L	1–1.5	0.047	0.003	X
A	1000	<i>Globobulimina</i> spp.	D	4–5	0.105	0.008	X

References

- IPCC. Summary for Policymakers. In *Climate Change 2022: Mitigation of Climate Change. Contribution of Working Group III to the Sixth Assessment Report of the Intergovernmental Panel on Climate Change*; Shukla, P.R., Skea, J., Slade, R., Al Khourdajie, A., van Diemen, R., McCollum, D., Pathak, M., Some, S., Vyas, P., Fradera, R., et al., Eds.; Cambridge University Press: Cambridge, UK; New York, NY, USA, 2022. [CrossRef]
- IPCC. Summary for Policymakers. Approved Synthesis Report of the IPCC Sixth Assessment Report (AR6). 2023. Available online: https://report.ipcc.ch/ar6syr/pdf/IPCC_AR6_SYR_SPM.pdf (accessed on 10 April 2017).
- EPICA community members. Eight glacial cycles from an Antarctic ice core. *Nature* **2004**, *429*, 623–628. [CrossRef] [PubMed]
- Henderson, G.M. New oceanic proxies for paleoclimate. *Earth Planet. Sci. Lett.* **2002**, *203*, 1–13. [CrossRef]
- Katz, M.E.; Cramer, B.S.; Franzese, A.; Honisch, B.; Miller, K.G.; Rosenthal, Y.; Wright, J.D. Traditional and emerging geochemical proxies in foraminifera. *J. Foraminif. Res.* **2010**, *40*, 165–192. [CrossRef]
- Lynch-Stieglitz, J.; Marchitto, T.M. Tracers of past ocean circulation. In *The Oceans and Marine Geochemistry*, 2nd ed.; Mottl, M.J., Elderfield, H., Eds.; Elsevier: Amsterdam, The Netherlands, 2014.
- Oomori, T. Distribution coefficient of Mg²⁺ ions between calcite and solutions at 10–50 °C. *Mar. Chem.* **1987**, *20*, 327. [CrossRef]
- Cusack, M.; Freer, A. Biomineralization: Elemental and Organic Influence in Carbonate Systems. *Chem. Rev.* **2008**, *108*, 4433–4454. [CrossRef] [PubMed]
- DeVilliers, S.; Greaves, M.; Elderfield, H. An intensity ratio calibration method for the accurate determination of Mg/Ca and Sr/Ca of marine carbonates by ICP-AES. *Geochem. Geophys. Geosyst.* **2002**, *3*, 2001GC000169. [CrossRef]
- Fernandez, D.P.; Gagnon, A.C.; Adkins, J.F. An Isotope Dilution ICP-MS Method for the Determination of Mg/Ca and Sr/Ca Ratios in Calcium Carbonate. *Geostand. Geoanalytical Res.* **2011**, *35*, 23–37. [CrossRef]
- Harding, D.J.; Arden, J.W.; Rickaby, R.E.M. A method for precise analysis of trace element/calcium ratios in carbonate samples using quadrupole inductively coupled plasma mass spectrometry. *Geochem. Geophys. Geosyst.* **2006**, *7*, Q06003. [CrossRef]
- Hathorne, E.C.; Alard, O.; James, R.H.; Rogers, N.W. Determination of intratest variability of trace elements in foraminifera by laser ablation inductively coupled plasma-mass spectrometry. *Geochem. Geophys. Geosyst.* **2003**, *4*, 8408. [CrossRef]
- Johnstone, H.J.H.; Yu, J.; Elderfield, H.; Schulz, M. Improving temperature estimates derived from Mg/Ca of planktonic foraminifera using X-ray computed tomography-based dissolution index, XDX. *Paleoceanography* **2011**, *26*, 17. [CrossRef]
- Marchitto, T.M. Precise multi-elemental ratios in small foraminiferal samples determined by sector field ICP-MS. *Geochem. Geophys. Geosyst.* **2006**, *7*, Q05P13. [CrossRef]
- Roman, M.; Ferretti, P.; Cairns, W.R.L.; Spolaor, A.; Turetta, C.; Barbante, C. High speed-low volume automated ICP-QMS method for determination of Mg/Ca in biogenic calcite. *J. Anal. At. Spectrom.* **2019**, *34*, 764–773. [CrossRef]
- Shen, C.C.; Chiu, H.Y.; Chiang, H.W.; Chu, M.F.; Wei, K.Y.; Steinke, S.; Chen, M.T.; Lin, Y.S.; Lo, L. High precision measurements of Mg/Ca and Sr/Ca ratios in carbonates by cold plasma inductively coupled plasma quadrupole mass spectrometry. *Chem. Geol.* **2007**, *236*, 339–349. [CrossRef]
- Yu, J.; Day, J.; Greaves, M.; Elderfield, H. Determination of multiple element/calcium ratios in foraminiferal calcite by quadrupole ICP-MS. *Geochem. Geophys. Geosyst.* **2005**, *6*, Q08P01. [CrossRef]
- Danelian, T.; Eynaud, F. Advances in micropaleontology: 60th anniversary special volume. *Rev. De Micropaleontol.* **2018**, *61*, 111–112. [CrossRef]

19. Erez, J. The source of ions for biomineralization in foraminifera and their implications for paleoceanographic proxies. *Biominer. Rev. Mineral. Geochem.* **2003**, *54*, 115–149. [[CrossRef](#)]
20. Jorissen, F.J.; De Stiger, H.C.; Widmark, J.G.V. A conceptual model explaining benthic foraminiferal microhabitats. *Mar. Micropaleontol.* **1995**, *26*, 3–15. [[CrossRef](#)]
21. Fontanier, C.; Jorissen, F.J.; Licari, L.; Alexandre, A.; Anschutz, P.; Carbonel, P. Live benthic foraminiferal faunas from the Bay of Biscay: Faunal density, composition, and microhabitats. *Deep-Sea Res. I* **2002**, *49*, 751–785. [[CrossRef](#)]
22. Elderfield, H.; Bertram, C.J.; Erez, J. Biomineralization model for the incorporation of trace elements into foraminiferal calcium carbonate. *Earth Planet. Sci. Lett.* **1996**, *142*, 409–423. [[CrossRef](#)]
23. Elderfield, H.; Ganssen, G. Past temperature and delta O-18 of surface ocean waters inferred from foraminiferal Mg/Ca ratios. *Nature* **2000**, *405*, 442–445. [[CrossRef](#)]
24. Lea, D.W.; Mashiotto, T.A.; Spero, H.J. Controls on magnesium and strontium uptake in planktonic foraminifera determined by live culturing. *Geochim. Cosmochim. Acta* **1999**, *63*, 2369–2379. [[CrossRef](#)]
25. Lea, D.W.; Pak, D.K.; Spero, H.J. Climate Impact of Late Quaternary Equatorial Pacific Sea Surface Temperature Variations. *Science* **2000**, *289*, 1719–1724. [[CrossRef](#)] [[PubMed](#)]
26. Lear, C.H.; Elderfield, H.; Wilson, P.A. Cenozoic Deep-Sea Temperatures and Global Ice Volumes from Mg/Ca in Benthic Foraminiferal Calcite. *Science* **2000**, *287*, 269–272. [[CrossRef](#)] [[PubMed](#)]
27. Barrientos, N.; Lear, C.H.; Jakobsson, M.; Stranne, C.; O'Regan, M.; Cronin, T.M.; Gukov, A.Y.; Coxall, H.K. Arctic Ocean benthic foraminifera Mg/Ca ratios and global Mg/Ca-temperature calibrations: New constraints at low temperatures. *Geochim. Cosmochim. Acta* **2018**, *236*, 240–259. [[CrossRef](#)]
28. Elderfield, H.; Yu, J.; Anand, P.; Kiefer, T.; Nyland, B. Calibrations for benthic foraminiferal Mg/Ca paleothermometry and the carbonate ion hypothesis. *Earth Planet. Sci. Lett.* **2006**, *250*, 633–649. [[CrossRef](#)]
29. Elderfield, H.; Greaves, M.; Barker, S.; Hall, I.R.; Tripathi, A.; Ferretti, P.; Crowhurst, S.; Booth, L.; Daunt, C. A record of bottom water temperature and seawater d¹⁸O for the Southern Ocean over the past 440 kyr based on Mg/Ca of benthic foraminiferal *Uvigerina* spp. *Quat. Sci. Rev.* **2010**, *29*, 160–169. [[CrossRef](#)]
30. Mawbey, E.M.; Hendry, K.H.; Greaves, M.J.; Hillenbrand, C.; Kuhn, G.; Spencer-Jones, C.L.; McClymont, E.L.; Vadman, K.J.; Shevenell, A.E.; Jernas, P.E.; et al. Mg/Ca-Temperature Calibration of Polar Benthic foraminifera species for reconstruction of bottom water temperatures on the Antarctic shelf. *Geochim. Cosmochim. Acta* **2020**, *283*, 54–66. [[CrossRef](#)]
31. Stirpe, C.R.; Allen, K.A.; Sikes, E.L.; Zhou, X.; Rosenthal, Y.; Cruz-Uribe, A.M.; Brooks, H.L. The Mg/Ca proxy for temperature: A *Uvigerina* core-top study in the Southwest Pacific. *Geochim. Cosmochim. Acta* **2021**, *309*, 299–312. [[CrossRef](#)]
32. Tisserand, A.A.; Dokken, T.M.; Waelbroeck, C.; Gherardi, J.-M.; Scao, V.; Fontanier, C.; Jorissen, F. Refining benthic foraminiferal Mg/Ca-temperature calibrations using core-tops from the western tropical Atlantic: Implication for paleotemperature estimation. *Geochem. Geophys. Geosyst.* **2013**, *14*, 929–946. [[CrossRef](#)]
33. Yu, Z.; Lei, Y.; Li, T.; Zhang, S.; Xiong, Z. Mg and Sr uptake in benthic foraminifera *Ammonia aomoriensis* based on culture and field studies. *Palaeogeogr. Palaeoclimatol. Palaeoecol.* **2019**, *520*, 229–239. [[CrossRef](#)]
34. Dissard, D.; Nehrke, G.; Reichart, G.J.; Bijma, J. The impact of salinity on the Mg/Ca and Sr/Ca ratio in the benthic foraminifera *Ammonia tepida*: Results from culture experiments. *Geochim. Cosmochim. Acta* **2010**, *74*, 928–940. [[CrossRef](#)]
35. Dissard, D.; Nehrke, G.; Reichart, G.J.; Bijma, J. Impact of seawater pCO₂ on calcification and Mg/Ca and Sr/Ca ratios in benthic foraminifera calcite: Results from culturing experiments with *Ammonia tepida*. *Biogeosciences* **2010**, *7*, 81–93. [[CrossRef](#)]
36. Evans, D.; Erez, J.; Oron, S.; Müller, W. Mg/Ca temperature and seawater-test chemistry relationships in the shallow-dwelling large benthic foraminifera *Operculina ammonoides*. *Geochim. Cosmochim. Acta* **2015**, *148*, 325–342. [[CrossRef](#)]
37. Filipsson, H.L.; Bernhard, J.M.; Lincoln, S.A.; McCorkle, D.C. A culture-based calibration of benthic foraminiferal paleotemperature proxies: Delta O-18 and Mg/Ca results. *Biogeosciences* **2010**, *7*, 1335–1347. [[CrossRef](#)]
38. Hintz, C.J.; Shaw, T.J.; Chandler, G.T.; Bernhard, J.M.; McCorkle, D.C.; Blanks, J.K. Trace/minor element: Calcium ratios in cultured benthic foraminifera. Part I: Inter-species and inter-individual variability. *Geochim. Cosmochim. Acta* **2006**, *70*, 1952–1963. [[CrossRef](#)]
39. Hintz, C.J.; Shaw, T.J.; Bernhard, J.M.; Chandler, G.T.; McCorkle, D.C.; Blanks, J.K. Trace/minor element: Calcium ratios in cultured benthic foraminifera. Part II: Ontogenetic variation. *Geochim. Cosmochim. Acta* **2006**, *70*, 1964–1976. [[CrossRef](#)]
40. Levi, A.; Müller, W.; Erez, J. Intrashell Variability of Trace elements in Benthic Foraminifera Grown under High CO₂ Levels. *Front. Earth Sci.* **2019**, *7*, 453029. [[CrossRef](#)]
41. Not, C.; Thibodeau, B.; Yokoyama, Y. Incorporation of Mg, Sr, Ba, U, and B in high-Mg calcite benthic foraminifera cultured under controlled pCO₂. *Geochem. Geophys. Geosyst.* **2018**, *19*, 83–98. [[CrossRef](#)]
42. Yu, J.; Elderfield, H. Mg/Ca in the benthic foraminifera *Cibicidoides wuellerstorfi* and *Cibicidoides mundulus*: Temperature versus carbonate ion saturation. *Earth Planet. Sci. Lett.* **2008**, *276*, 129–139. [[CrossRef](#)]
43. Barker, S.; Greaves, M.; Elderfield, H. A study of cleaning procedures used for foraminiferal Mg/Ca paleothermometry. *Geochem. Geophys. Geosyst.* **2003**, *4*, 8407. [[CrossRef](#)]
44. Yu, J.; Elderfield, H.; Greaves, M.; Day, J. Preferential dissolution of benthic foraminiferal calcite during laboratory reductive cleaning. *Geochem. Geophys. Geosyst.* **2007**, *8*, Q06016. [[CrossRef](#)]
45. Lorens, R.B. Sr, Cd, Mn and Co distribution coefficients in calcite as a function of calcite precipitation rate. *Geochim. Cosmochim. Acta* **1981**, *45*, 553–561. [[CrossRef](#)]

46. Morse, J.W.; Bender, M.L. Partition coefficients in calcite: Examination of factors influencing the validity of experimental results and their application to natural systems. *Chem. Geol.* **1990**, *82*, 265–277. [CrossRef]
47. Tang, J.; Köhler, S.J.; Dietzel, M. Sr²⁺/Ca²⁺ and ⁴⁴Ca/⁴⁰Ca fractionation during inorganic calcite formation: I. Sr incorporation. *Geochim. Cosmochim. Acta* **2008**, *72*, 3718–3732. [CrossRef]
48. Mojtahid, M.; Depuydt, P.; Mouret, A.; Le Houedec, S.; Fiorini, S.; Chollet, S.; Massol, F.; Dohou, F.; Filipsson, H.; Boer, W.; et al. Assessing the impact of different carbonate system parameters on benthic foraminifera from controlled growth experiments. *Chem. Geol.* **2023**, *623*, 121396. [CrossRef]
49. Raitzsch, M.; Dueñas-Bohórquez, A.; Reichart, G.-J.; de Nooijer, L.J.; Bickert, T. Incorporation of Mg and Sr in calcite of cultured benthic foraminifera: Impact of calcium concentration and associated calcite saturation state. *Biogeosciences* **2010**, *7*, 869–881. [CrossRef]
50. Ma, R.; Sepulcre, S.; Bassinot, L.; Haurine, F.; Tisnérat-Laborde, N.; Colin, C. North Indian Ocean circulation since the last deglaciation as inferred from new elemental ratio records for benthic foraminifera *Hoeglundina elegans*. *Paleoceanogr. Paleoclimatol.* **2020**, *35*, e2019PA003801. [CrossRef]
51. Yu, J.; Elderfield, H.; Jin, Z.; Tomascak, P.; Rohling, E.J. Controls on Sr/Ca in benthic foraminifera and implications for seawater Sr/Ca during the late Pleistocene. *Quat. Sci. Rev.* **2014**, *98*, 1–6. [CrossRef]
52. Rosenthal, Y.; Boyle, E.A.; Slowey, N. Temperature control on the incorporation of magnesium, strontium, fluorine, and cadmium into benthic foraminiferal shells from Little Bahama Bank: Prospects for thermocline paleoceanography. *Geochim. Cosmochim. Acta* **1997**, *61*, 3633–3643. [CrossRef]
53. Lynch-Stieglitz, J.; Adkins, J.F.; Curry, W.B.; Dokken, T.; Hall, I.R.; Herguera, J.C.; Hirschi, J.J.-M.; Ivanova, E.V.; Kissel, C.; Marchal, O.; et al. Atlantic Meridional Overturning Circulation during the Last Glacial Maximum. *Science* **2007**, *316*, 66–69. [CrossRef]
54. Lynch-Stieglitz, J. The Atlantic Meridional Overturning Circulation and Abrupt Climate Change. *Annu. Rev. Mar. Sci.* **2017**, *9*, 83–104. [CrossRef] [PubMed]
55. Mojtahid, M.; Griveaud, C.; Fontanier, C.; Anschutz, P.; Jorissen, F.J. Live benthic foraminiferal faunas along a bathymetrical transect (140–4800 m) in the Bay of Biscay (NE Atlantic). *Rev. Micropaleontol.* **2010**, *53*, 139e162. [CrossRef]
56. Lewis, E.; Wallace, D. CO2SYS.EXE, Program Developed for CO₂ System Calculations; Brookhaven National Laboratory and Institut für Meereskunde: Hamburg, Germany, 2000. Available online: <http://cdiac.esd.ornl.gov/oceans/co2rprt.html> (accessed on 10 April 2017).
57. Schlitzer, R. Electronic Atlas of WOCE Hydrographic and Tracer Data Now Available. *Eos T. Am. Geophys. Un.* **2000**, *81*, 45. [CrossRef]
58. Tréguer, P.; Le Corre, P.; Grall, J.R. The seasonal variations of nutrients in the upper waters of the Bay of Biscay region and their relation to phytoplanktonic growth. *Deep-Sea Res.* **1979**, *26*, 1121–1152. [CrossRef]
59. Van Aken, H.M. The hydrography of the mid-latitude northeast Atlantic Ocean: The thermocline water mass. *Deep-Sea Res. I* **2000**, *48*, 237–267. [CrossRef]
60. Van Aken, H.M. The hydrography of the mid-latitude Northeast Atlantic Ocean: The deep water masses. *Deep-Sea Res. I* **2000**, *47*, 757–788. [CrossRef]
61. Van Aken, H.M. The hydrography of the mid-latitude Northeast Atlantic Ocean: The intermediate water masses. *Deep-Sea Res. I* **2000**, *47*, 789–824. [CrossRef]
62. McCorkle, D.C.; Martin, P.A.; Lea, D.W.; Klinkhammer, G.P. Evidence of a Dissolution Effect on Benthic Foraminiferal Shell Chemistry—Delta-C-13, Cd/Ca, Ba/Ca, and Sr/Ca Results from the Ontong Java Plateau. *Paleoceanography* **1995**, *10*, 699–714. [CrossRef]
63. Mojtahid, M.; Jorissen, F.J.; Garcia, J.; Schiebel, R.; Michel, E.; Eynaud, F.; Gillet, H.; Cremer, M.; Diz Ferreiro, P.; Siccha, M.; et al. High resolution Holocene record in the southeastern Bay of Biscay: Global versus regional climate signals. *Palaeogeogr. Palaeoclimatol. Palaeoecol.* **2013**, *377*, 28–44. [CrossRef]
64. Fontanier, C.; Jorissen, F.J.; Chaillou, G.; David, C.; Anschutz, P.; Lafon, V. Seasonal and interannual variability of benthic foraminiferal faunas at 550 m depth in the Bay of Biscay. *Deep-Sea Res. I* **2003**, *50*, 457–494. [CrossRef]
65. Walton, W.R. Techniques for recognition of living Foraminifera. *Contrib. Cushman Found. Foraminifer. Res.* **1952**, *3*, 56–60.
66. Coadic, R.; Bassinot, F.; Douville, E.; Michel, E.; Dissard, D.; Greaves, M. A core-top study of dissolution effect on B/Ca in Globigerinoides sacculifer from the tropical Atlantic: Potential bias for paleo-reconstruction of seawater carbonate chemistry. *Geochem. Geophys. Geosyst.* **2013**, *14*, 1053–1068. [CrossRef]
67. Rosenthal, Y.; Lear, C.H.; Oppo, D.W.; Linsley, B.K. Temperature and carbonate ion effects on Mg/Ca and Sr/Ca ratios in benthic foraminifera: Aragonitic species *Hoeglundina elegans*. *Paleoceanography* **2006**, *21*. [CrossRef]
68. Allison, N.; Austin, W.E.N. Serial Mg/Ca and Sr/Ca chronologies across single benthic foraminifera tests. *Chem. Geol.* **2008**, *253*, 83–88. [CrossRef]
69. Kristjánsdóttir, G.B.; Lea, D.W.; Jennings, A.E.; Pak, D.K.; Belanger, C. New spatial Mg/Ca-temperature calibrations for three Arctic, benthic foraminifera and reconstruction of north Iceland shelf temperature for the past 4000 years. *Geochem. Geophys. Geosyst.* **2007**, *8*, Q03P21. [CrossRef]

70. Hasenfratz, A.P.; Schiebel, R.; Thornalley, D.J.R.; Schönfeld, J.; Jaccard, S.L.; MartínezGarcía, A.; Holbourn, A.; Jennings, A.E.; Kuhnt, W.; Lear, C.H.; et al. Mg/Ca-temperature calibration for the benthic foraminifera *Melonis barleeanum* and *Melonis pompilioides*. *Geochim. Cosmochim. Acta* **2017**, *217*, 365–383. [[CrossRef](#)]
71. Skinner, L.C.; Shackleton, N.J.; Elderfield, H. Millennial-scale variability of deep-water temperature and $\delta^{18}\text{O}_{\text{dw}}$ indicating deep-water source variations in the Northeast Atlantic, 0–34 cal. ka BP. *Geochem. Geophys. Geosyst.* **2003**, *4*, 1098. [[CrossRef](#)]
72. Rosenthal, Y.; Perron-Cashman, S.; Lear, C.H.; Bard, E.; Barker, S.; Billups, K.; Bryan, M.; Delaney, M.L.; Dwyer, G.S.; Elderfield, H.; et al. Interlaboratory comparison study of Mg/Ca and Sr/Ca measurements in planktonic foraminifera for paleoceanographic research. *Geochem. Geophys. Geosyst.* **2004**, *5*, Q04D09. [[CrossRef](#)]
73. Keul, N.; Langer, G.; Thoms, S.; De Nooijer, L.J.; Reichert, G.; Bijma, J. Exploring foraminiferal Sr/Ca as a new carbonate system proxy. *Geochim. Cosmochim. Acta* **2017**, *202*, 374–386. [[CrossRef](#)]
74. Boyle, E.A.; Keigwin, L.D. Comparison of Atlantic and Pacific paleochemical records for the last 215,000 years: Changes in deep ocean circulation and chemical inventories. *Earth Planet. Sci. Lett.* **1985**, *76*, 135–150. [[CrossRef](#)]
75. Pak, D.K.; Lea, D.W.; Kennett, J.P. A sediment trap time series of foraminiferal Mg/Ca and $\delta^{18}\text{O}$. *Eos Trans. AGU* **2000**, *81*, F662.
76. Anand, P.; Elderfield, H.; Conte, M.H. Calibration of Mg/Ca thermometry in planktonic foraminifera from a sediment trap time series. *Paleoceanography* **2003**, *18*, 1050. [[CrossRef](#)]
77. Pak, D.K.; Lea, D.W.; Kennett, J.P. Seasonal and interannual variation in Santa Barbara Basin water temperatures observed in sediment trap foraminiferal Mg/Ca. *Geochem. Geophys. Geosyst.* **2004**, *5*, Q12008. [[CrossRef](#)]
78. Bryan, S.P.; Marchitto, T.M. Mg/Ca-temperature proxy in benthic foraminifera: New calibrations from the Florida Straits and a hypothesis regarding Mg/Li. *Paleoceanography* **2008**, *23*, PA2220. [[CrossRef](#)]
79. Martin, W.R.; Sayles, F.L. CaCO_3 dissolution in sediments of the Ceara Rise, western equatorial Atlantic. *Geochim. Cosmochim. Acta* **1996**, *60*, 243–263. [[CrossRef](#)]
80. Martin, W.R.; Sayles, F.L. Organic matter oxidation in deep-sea sediments: Distribution in the sediment column and implications for calcite dissolution. *Deep-Sea Res. II* **2006**, *53*, 771–792. [[CrossRef](#)]

Disclaimer/Publisher’s Note: The statements, opinions and data contained in all publications are solely those of the individual author(s) and contributor(s) and not of MDPI and/or the editor(s). MDPI and/or the editor(s) disclaim responsibility for any injury to people or property resulting from any ideas, methods, instructions or products referred to in the content.